Radiation and Scattering of an Arbitrarily Flanged Dielectric-Loaded Waveguide

Radiation and Scattering of an Arbitrarily Flanged Dielectric-Loaded Waveguide

Vito Daniele, Guido Lombardi, *Senior Member, IEEE*, Rodolfo S. Zich, *Honorary Member, IEEE*

***Abstract*—In this paper, we present a new methodology in spectral domain to study novel complex canonical electromagnetic problems constituted of perfectly electrically conducting (PEC) wedges immersed in complex environments. In particular we present an arbitrarily flanged dielectric-loaded waveguide (Fig. 1) that may resemble practical structures in scattering analysis, radar applications, antenna's design and electromagnetic compatibility. The proposed method is based on the recent developed semi-analytical method known as Generalized Wiener-Hopf Technique (GWHT) that extends the applicability of classical Wiener-Hopf method to a new variety of problems constituted of different geometries and materials. In this paper the method is further extended and it is now capable of handling piecewise constant inhomogeneous dielectric layers by resorting to the application of characteristic Green's function procedure starting from the wave equation. The method has the benefit to be a comprehensive mathematical model and to be quasi-analytical thus it allows to investigate the true physics of the problem in terms of field's components. The proposed solution is of interest in computational electromagnetics also to benchmark numerical codes. Validation through numerical results is reported in terms of engineering quantities such as GTD/UTD diffraction coefficients, total far fields and modal fields.**

***Index Terms*—Wedges, Grounded Dielectric Slab, Flanged Dielectric-Loaded Waveguide, Inhomogeneous Material, Wiener-Hopf method, Green's function, Integral equations, Near-field interactions, Electromagnetic diffraction, Scattering, Radar, Antenna technologies, EMC, Network Modelling.**

I. Introduction

THE accurate and efficient study of radiation and scattering from complex wedge structures is of great interest in electromagnetic engineering communities in particular in the field of antenna's design, radar applications and electromagnetic compatibility. In computational electromagnetics particular attention is dedicated to the correct modelling of near-field interaction among thin structures, dielectric interfaces and edges of wedges.

{\rm word}

In this paper we propose a novel complex canonical electromagnetic problem constituted of a perfectly electrically conducting (PEC) wedge lying on an grounded half-dielectric slab as reported in Figs. 1: an arbitrarily flanged dielectric-loaded parallel PEC plate waveguide. Both cartesian and cylindrical coordinates are used to describe the problem. The origin O is located at the edge of the PEC wedge for coordinates (x, y, z) and (ρ, φ, z). The PEC wedge is defined by $\rho > 0, \Phi < \varphi < \pi$ and the grounded half-dielectric slab is delimited by $-d < y < 0$. Both structures are with symmetry axis along the z. In Figs. 1, the two sub-figures look different in terms of applications. In particular, sub-figure (a) resembles scattering analysis for example in radar applications such as inlets in aerospace engineering, while sub-figure (b) can model an antenna problem similar to a horn fed by a waveguide loaded by a dielectric material.

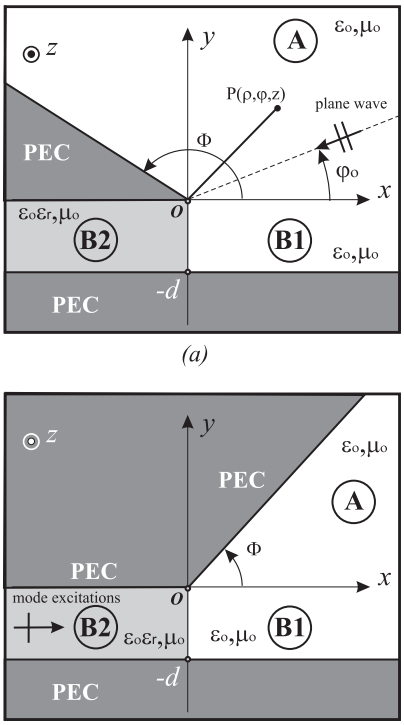

Fig. 1: The PEC wedge lying on a grounded half-dielectric slab illuminated by a plane wave or fed by a modal field, i.e. an arbitrarily flanged dielectric-loaded waveguide: case (a) with aperture angle $\Phi > \pi/2$ resembles scattering analysis for example in radar applications such as inlets in aerospace engineering, case (b) with aperture angle $\Phi < \pi/2$ resembles antenna problem as horn structures fed by waveguide loaded by dielectric material. Cartesian coordinates (x, y, z) and cylindrical coordinates (ρ, φ, z) centered in O are reported in the figures to describe the problem.

Two regions are defined: region *A* and region *B*. Region *A* is a homogenous angular region delimited by $0 < \varphi < \Phi$ and characterized by free space impedance $Z_o = \sqrt{\mu_o/\varepsilon_o}$ and propagation constant $k = \omega\sqrt{\mu_o\varepsilon_o}$. Region *B* is a grounded

Manuscript received —; revised —. Version: November 28, 2019

This work was supported in part by Politecnico di Torino and by Links Foundation, Turin, Italy. (Corresponding author: Guido Lombardi.) The authors are with Politecnico di Torino, Corso Duca degli Abruzzi 24, 10129 Torino, Italy, and also with Links Foundation, 10138 Turin, Italy (email: vito.daniele@polito.it, guido.lombardi@polito.it, rodolfo.zich@torinowireless.it).

inhomogeneous dielectric slab region better described by two subregions: subregion *B2* is with rectangular shape delimited by $x < 0$, $-d < y < 0$ and characterized by relative dielectric permittivity ε_r, while subregion *B1* is in free space with rectangular shape delimited by $x > 0$, $-d < y < 0$ and homogenous to region *A*. PEC interfaces and related boundary conditions are located at 1) $\rho > 0$, $\varphi = \Phi$, 2) $x < 0$, $y = 0$, 3) $y = -d$; while at $x = 0$, $-d < y < 0$ is located a free-space/dielectric interface.

In the following time harmonic electromagnetic field is assumed with a time dependence specified by $e^{+j\omega t}$ which is suppressed. For the sake of simplicity, the structure is studied considering E_z polarization, however generalization to H_z polarization or skew incident case is possible and it doubles the equations. The structure is analyzed considering two kind of sources: illumination by plane waves from region *A* and feeding the dielectric loaded parallel PEC plate waveguide *B2* with modal fields.

In this paper we propose a new comprehensive mathematical model in spectral domain that takes into account the entire structure in one shot. The method is based on an extension of the classical Wiener-Hopf method [1]-[10] that is a well established technique to solve problems with discontinuities in all branches of physics and applied mathematics and, recent developments of this technique done by other authors are reported in [11]-[23]. A brief historical perspective is available in [24] and a nice reference list is reported in [25].

Recently, the authors of this paper have introduced the Generalized Wiener-Hopf Technique (GWHT) that is a novel effective technique to handle angular regions such as isolated impenetrable and penetrable wedge problems [26]-[33]. According to the authors' opinion, the GWHT together with the Sommerfeld-Malyuzhinets (SM) technique (see [34]-[38] and reference therein) and the methods based on the Kontorovich-Lebedev (KL) transform (see [39]-[41] and reference therein) completes the spectral techniques capable to deal with isolated wedge problems. Now, the GWHT is further extended and able to deal with new complex electromagnetic problems constituted of sub-regions of different materials and shapes, i.e. angular and rectangular/layer regions [42]-[47],[25].

Typically the method starts from the deduction of Generalized Wiener-Hopf equations (GWHEs) for each of the regions that constitute the complex problem. Each subregion is canonical in geometry and homogenous in material, as for example angular region *A* of Fig. 1 and layered regions. The GWHEs of homogenous angular regions are derived using radial Laplace transforms of field components and the characteristic Green's function procedure as described in [26]-[27]. The equations are considered generalized versions for Wiener-Hopf technique since the plus and minus unknows are defined into different complex planes. According to the classical spectral theory of homogeneous layered regions based on transmission line modeling [48],[10], spectral equations are obtained for the bilateral Laplace transforms of field components that are rephrased into unilateral transforms to be used in the GWHT. However, in the proposed problem, region *B* is constituted of two materials and it will requires special effort as described in details in this paper. Following the procedure reported in this paper it is now possible to study piecewise constant inhomogeneous dielectric layers by resorting again to the application of characteristic Green's function procedure starting from the wave equation.

The system of spectral equations usually does not allow a closed form solution following the classical scheme of Wiener-Hopf technique based on 1) the multiplicative factorization of the kernel, 2) the additive decomposition of functions and 3) the application of Liouville's Theorem. An effective approximate semi-analytical technique to obtain the solution of system of GWHEs is the *Fredholm Factorization* [49], [10] that reduces the system of GWHEs to integral representations by eliminating one kind of unknowns (plus or minus) via contour integration. The application in the context of wedge diffraction is reported in [27]-[33],[42]-[46]. The coupling of integral representations yields a system of Fredholm integral equations of second kind amenable of approximate solution via simple discretization [50]. A complete solution of the original system of GWHEs is obtained by reconstructing all the unknowns through the integral representations and the same GWHEs. Analytic continuation in complex plane of the approximate solution is obtained by rephrasing the original GWHEs to difference equations. The solution of the method are spectral quantities (WH unknowns) that contain the global information of fields in terms of spectra. The quasi-analytical solution can be analyzed in terms of field components via inverse spectral transformation and asymptotics (see for instance [45]-[46]) and engineering parameters can be retrieved. Taking inspiration from [48], [51], [10], [44], the integral representations of each region can be interpreted as equivalent network. This formalism and pictorial representation orders and systematizes the procedure to obtain the spectral equations and the integral representations for complex problems avoiding redundancy, see for example [44],[45]-[46],[25].

The literature shows several works related to the structure proposed in this paper with recent applications, see [5],[52]-[62] and reference therein. However, we assert that our method has the benefit to model the entire structure with a true comprehensive mathematical model in spectral domain that avoids multiple steps of interaction among separated objects like in ray-tracing with multiple diffraction coefficients or like in iterative physical optics. The main result is the true spectra of field components along observation directions. Moreover the method is independent from the thickness, the density of the materials and the distance between the objects.

The paper is organized into 7 Sections and an Appendix. In Section II we introduce the formulation of the problem and the mathematical background preparatory for the GWHEs reported in Section III. Section IV presents how to reduce the system of GWHEs to integral representations via Fredholm factorization and illustrates how to couple the integral representations to obtain a Fredholm integral equation (FIE) of second kind for the solution of the problem. In the same Section the network paradigm is introduced to facilitate deduction of the equations in complex problems. Analytic continuation of the approximate solution is presented in Appendix A and it is propaedeutical to Section V where we estimate physical/engineering quantities as GTD/UTD diffrac-

tion coefficients, total far fields and modal field. Section VI provides validation and convergence of the proposed method and it compares our results with the ones obtained by a fully numerical technique embedding singular modelling [63],[64]-[66], thus demonstrating the superiority of the proposed semi-analytical technique for canonical problems (with infinite geometry) with respect to the case of finite structure. Conclusions are reported in the last Section.

II. Formulation of the Problem, Spectral Unknowns and Mathematical Background

With reference to Figs. 1, at E_z polarization, the non-null field components $E_z(x,y), H_x(x,y), H_y(x,y)$ are independent from z and are governed by the wave equation (in the following z dependence is omitted).

According to the coordinate systems and the notation described in Section I, the boundary conditions of PEC interfaces are: $E_z(\rho,\varphi=\Phi)=0$, $E_z(\rho,\varphi=\pi)=0$ and $E_z(x,y=-d)=0$. The problem shows continuity of E_z, H_y at the free space/dielectric interface $x=0$, $-d<y<0$ between subregions *B1* and *B2*, i.e. $E_z(x=0_-,y)=E_z(x=0_+,y)$, $H_y(x=0_-,y)=H_y(x=0_+,y)$ with $-d<y<0$. Moreover according to definition reported in Section I the problem shows continuity also at the interface located between region *A* and *B1*, i.e. $E_z(x,y=0_-)=E_z(x,y=0_+)$, $H_x(x,y=0_)=H_x(x,y=0_+)$ with $x>0$. Near the edge as $\rho\to 0$, $E_z(\rho,\varphi)$ remains finite (Meixner's edge condition [63]): $E_z(\rho,\varphi)=M_0+O(\rho^m)$ with constant M_0 and $m>0$. In region *A* (and similarly in *B1*) the following radiation condition holds: $\left|E_z(\rho,\varphi)-E_z^{GO}(\rho,\varphi)\right|\le e^{-a\rho}$ with $a>0$ and where E_z^{GO} is the total Geometrical Optics components of E_z. In region *B2* the following modal condition holds: $\left|E_z(x,y)-E_z^{INC}(x,y\right|\le e^{-b_2 x}$ with $b_2>0$ and where E_z^{INC} is the total modal progressive (toward positive x) incident field component of E_z. According to the uniqueness theorem, the solution fulfills the edge, the radiation and the modal conditions.

The formulation of the problem in the spectral domain is based on the definition of the radial Laplace transforms

$$\begin{cases} V_+(\sigma,\varphi)=\int_0^\infty E_z(\rho,\varphi)e^{j\sigma\rho}d\rho \\ I_+(\sigma,\varphi)=\int_0^\infty H_\rho(\rho,\varphi)e^{j\sigma\rho}d\rho \end{cases}, \quad (y\ge 0) \tag{1}$$

and on the definition of the bilateral Laplace transforms

$$\begin{cases} v(\eta,y)=\int_{-\infty}^{\infty} E_z(x,y)e^{j\eta x}dx \\ i(\eta,y)=\int_{-\infty}^{\infty} H_x(x,y)e^{j\eta x}dx \end{cases}, \quad (-d\le y\le 0) \tag{2}$$

The axial spectral unknowns (3) will be used as reference unknowns to obtain the GWHEs of the problem:

$$\begin{aligned} &V_+(\eta)=V_+(\sigma=\eta,\varphi=0),\ I_+(\eta)=I_+(\sigma=\eta,\varphi=0) \\ &V_{\pi+}(\eta)=V_+(\sigma=\eta,\varphi=\pi),\ I_{\pi+}(\eta)=I_+(\sigma=\eta,\varphi=\pi) \end{aligned} \tag{3}$$

with the definition of related minus functions $V_-(\eta)=V_{\pi+}(-\eta)$ and $I_-(\eta)=-I_{\pi+}(-\eta)$. From (1)-(3) we note that the Laplace transforms and the bilateral Laplace transforms at the interface $y=0$ are related together:

$$\begin{cases} v(\eta,y=0)=V_+(\eta)+V_{\pi+}(-\eta) \\ i(\eta,y=0)=I_+(\eta)-I_{\pi+}(-\eta) \end{cases} \tag{4}$$

with $V_{\pi+}(-\eta)=0$ due to the PEC boundary condition of the problem under investigation.

Furthermore, to obtain the GWHEs of the angular region *A*, we need to define the radial Laplace transform of the magnetic field along the PEC face of the wedge (face spectral unknown):

$$I_{a+}(-m)=\int_0^\infty H_\rho(\rho,\varphi=\Phi)e^{-jm\rho}d\rho=I_+(\sigma=-m,\varphi=\Phi) \tag{5}$$

No face spectrum is present for E_z component due to the PEC boundary condition ($V_{a+}(-m)=0$).

To clarify the notation, with reference to the η complex plane, the spectral unknowns are labeled with $\pm$ subscripts: $+$ indicates plus functions in the η complex plane, *i.e.* analytic functions in η that are regular in an upper half-plane ($Im[\eta]>Im[\eta_{up}]$) and goes to zero at infinity; conversely $-$ indicates minus functions in the η complex plane, *i.e.* analytic functions in η that are regular in a lower half-plane ($Im[\eta]<Im[\eta_{lo}]$) and goes to zero at infinity. The $+$ ($-$) functions are considered non-conventional, i.e. non-standard, if $Im[\eta_{up}]>0$ ($Im[\eta_{lo}]<0$). As commonly done in WH technique, we assume small vanishing losses in the medium to avoid singularities of the sources in the real axis of the spectral plane: $k=k_r-jk_i$ where $k_r,k_i>0$ and $k_i<<k_r$. In fact either plane waves or modal field excitations generate poles in the spectra, as illustrated below.

In the following we use a generalization of the classical Cauchy decomposition formula for WH unknowns [10] in presence of non standard poles:

$$\begin{aligned} &\tfrac{1}{2\pi j}\int_{\gamma_{1\eta}}\tfrac{F_+(\eta')}{\eta'-\eta}d\eta'=F_+(\eta)-F_+^{ns}(\eta), \quad \tfrac{1}{2\pi j}\int_{\gamma_{2\eta}}\tfrac{F_+(\eta')}{\eta'-\eta}d\eta'=-F_+^{ns}(\eta) \\ &\tfrac{1}{2\pi j}\int_{\gamma_{2\eta}}\tfrac{F_-(\eta')}{\eta'-\eta}d\eta'=-F_-(\eta)+F_-^{ns}(\eta), \quad \tfrac{1}{2\pi j}\int_{\gamma_{1\eta}}\tfrac{F_-(\eta')}{\eta'-\eta}d\eta'=F_-^{ns}(\eta) \end{aligned} \tag{6}$$

for $\eta\in\mathbb{R}$ and where $F_+^{ns}(\eta)$ and $F_-^{ns}(\eta)$ are the non-standard part of $F_+(\eta)$ and $F_-(\eta)$. In (6) $\gamma_{1\eta}$ and $\gamma_{2\eta}$ are respectively the *smile* and the *frown* integration line in η-plane [49],[10], i.e. the real axis of η'-plane indented at $\eta'=\eta$ with a small semi-circumference respectively in the lower and in the upper half plane.

In the present problem we notice that the non-standard parts are related only to Geometrical Optics (GO) components or modal fields with infinite geometrical support (property of Laplace transform) that can be controlled a priori. In case of plane wave illumination at E_z polarization, we denote the azimuthal direction of GO waves with φ_{go} where the subscripts go are in lower case (upper case) if referred to a ingoing (outgoing) wave towards (from) the edge of the wedge (with $\varphi_{GO}=\varphi_{go}\pm\pi$):

$$E_z^{go}(\rho,\varphi)=E_{go}e^{jk\,\rho\cos(\varphi-\varphi_{go})} \tag{7}$$

In case of modal excitation, we consider the representation of the field in region *B2* expanded into x-progressive TE_n modes

$$E_z{}^{(n)}(x,y) = E_{on}\sin\left(\frac{n\pi}{d}y\right)e^{-j\chi_n x} \tag{8}$$

with longitudinal propagation constant of the parallel PEC plate waveguide of size d filled by dielectric medium

$$\chi_n = \sqrt{k_d^2 - \left(\frac{n\pi}{d}\right)^2} \tag{9}$$

where $k_d = k\sqrt{\varepsilon_r}$. Note that the Laplace transforms of (7) and (8) yields poles in spectral planes that can generate non-standard components in the spectral unknowns in relation to the kind of unknown (minus/plus), the complex plane to be considered (for example σ, η, m) and the physical parameters of the excitations. For example an incident plane wave with incident angle φ_o generates a pole $\eta_o = -k\cos(\varphi_o)$ in the axial spectrum $V_+(\eta)$ defined in the η plane whose location depends on the incident angle φ_o (i.e. η_o is in the 2nd quadrant if $0 < \varphi_o < \pi/2$ or 4th quadrant if $\pi/2 < \varphi_o < \pi$ along the segment that connects k to $-k$). In the following we will need to pay particular attention to the singularities of the sources since the GWHEs, that will be introduced, are defined in terms of multivariate functions that depends on the spectral propagation constant $\tau_1(\eta) = \sqrt{k^2 - \eta^2}$. In this case the definition of non-standard poles needs also to be related to the proper sheet of the functions introduced in the problem: in this case we consider as proper sheet the one with $\tau_1(0) = k$ and we assume standard vertical branch lines from $\eta = \pm k$.

III. The GWHEs of the Problem

Typically the method starts from the deduction of Generalized Wiener-Hopf equations (GWHEs) for each region/subregion that constitute the complex problem. Each subregion needs to be canonical in geometry and homogenous in material. Based on the definitions reported in Section II, subsections A and B reports the GWHEs of the problem at E_z polarization respectively for regions *A* and *B*.

A. Region A

The GWHE of region *A* is obtained following the theory for angular regions reported in [26]-[27] and using the definitions of the axial spectral unknowns (3) and the face spectral unknown (5):

$$Y_c(\eta)\,V_+(\eta) - I_+(\eta) = -I_{a+}(-m(\eta)) \tag{10}$$

where $Y_c(\eta) = \frac{1}{Z_c(\eta)} = \frac{\tau_1(\eta)}{kZ_o}$ is the free-space spectral admittance defined in terms of the free space impedance $Z_o = 1/Y_o$ and the free-space spectral propagation constant $\tau_1(\eta) = \sqrt{k^2 - \eta^2}$.

Eq. (10) is a generalized version of Wiener-Hopf equation because the plus functions are defined in the η complex plane, while $I_{a+}(-m(\eta))$ is a minus function in the m complex plane. The two complex planes are related together by

$$m(\eta) = -\eta\cos\Phi + \tau_1(\eta)\sin\Phi \tag{11}$$

The mapping (12) allows to reduce (10) to a classical WH equation with the definition of the new $\alpha(\eta)$ complex plane [26]-[27]:

$$\alpha(\eta) = -k\cos\left(\frac{\pi}{\Phi}\arccos\left(-\frac{\eta}{k}\right)\right) \tag{12}$$

We assume the proper sheet of the mapping the one with $\alpha(0) = -k\cos(\frac{\pi^2}{2\Phi})$ and the branch lines to be considered are such that the contour integrations reported in the procedure of Section IV-A do not intersect them. An important property is that plus functions in η plane and minus functions in m plane preserve their regularity half plane in α plane but this property does not hold for minus functions in η and plus functions in m. Note that these last two functions are not present in (10).

B. Region B

The grounded half-dielectric slab is an inhomogeneous region constituted of subregion *B1* and *B2*. In this case, the GWHE is obtained via the following steps: 1) split the region *B* into the two homogenous subregions as in Figs. 1, 2) apply the Laplace transforms to the basic wave equations, 3) use the modal representation of fields in the subregions.

The wave equations of the two subregions are:

$$\left(\frac{\partial^2}{\partial x^2} + \frac{\partial^2}{\partial y^2} + k_n^2\right)E_z(x,y) = 0,\ n = 1,2 \tag{13}$$

with $k_1 = k$ and $k_2 = k_d$. Applying the Laplace transform to E_z

$$\begin{aligned}\tilde{E}_z(\eta,y) &= \textstyle\int_0^\infty E_z(x,y)e^{j\eta x}dx,\ in\,B1\\ \tilde{E}_z(\eta,y) &= \textstyle\int_{-\infty}^0 E_z(x,y)e^{j\eta x}dx,\ in\,B2\end{aligned} \tag{14}$$

(13) become

$$\left(\frac{d^2}{dy^2} + \tau_n^2\right)\tilde{E}_z(\eta,y) = f_n(\eta,y),\ n = 1,2 \tag{15}$$

where $\tau_n(\eta) = \sqrt{k_n^2 - \eta^2}$ and with

$$f_n(\eta,y') = \mp j\eta E_z(0_\pm,y) \pm \frac{\partial}{\partial x}E_z(0_\pm,y) \tag{16}$$

$$\frac{\partial}{\partial x}E_z(0_\pm,y) = +j\omega\mu_o H_y(0_\pm,y) \tag{17}$$

assuming the notation $\frac{\partial}{\partial x}E_z(a,y) = \frac{\partial}{\partial x}E_z(x,y)\big|_{x=a}$, $\pm$ sign is plus(minus) for $n = 1(2)$ and the opposite assumption holds for $\mp$ sign.

Eqs. (15) are particular versions of the Sturm-Liouville problem with non-homogenous boundary conditions [67],[51]. By applying the characteristic Green's function procedure to (15) in subregion *B1* ($n = 1$) we obtain the particular integral

$$\tilde{E}_z^{(part)}(\eta,y) = \int_{-d}^{0} g_\eta(y,y')f_1(\eta,y')dy' \tag{18}$$

with the Green's function

$$g_\eta(y,y') = \frac{\overleftarrow{\varphi}_\eta(y_<)\vec{\varphi}_\eta(y_>)}{W_r\left[\overleftarrow{\varphi}_\eta(y),\vec{\varphi}_\eta(y)\right]} \tag{19}$$

where $W_r\left[\overleftarrow{\varphi}_\eta(y),\vec{\varphi}_\eta(y)\right]$ is the Wronskian of the two functions $\overleftarrow{\varphi}_\eta(y)$ and $\vec{\varphi}_\eta(y)$ and $y_<$ and $y_>$ denote respectively the lesser and the greater of quantities y and y'. Note that $\overleftarrow{\varphi}_\eta(y)$ and $\vec{\varphi}_\eta(y)$ are solutions of (15) with $n = 1$ satisfying the boundary conditions, in particular the PEC boundary condition at $y = -d$. We select the following two functions to continue the procedure

$$\begin{aligned}\overleftarrow{\varphi}_\alpha(y) &= \sin\left[\tau_1(y+d)\right]\\ \vec{\varphi}_\alpha(y) &= \cos\left(\tau_1 y\right)\end{aligned} \tag{20}$$

and we note that the Wronskian is, in this case, the constant $-\tau_1 \cos(\tau_1 d)$; thus

$$g_\eta(y,y') = -\frac{\cos(\tau_1 y_>)\sin(\tau_1(y_< + d))}{\tau_1 \cos(\tau d)} \tag{21}$$

By substituting (16) and (21) into (18) we obtain an explicit expression of the particular integral. The solution of homogenous version of (15) with PEC boundary condition at $y=-d$ is of the form

$$\tilde{E}_z^{(hom)}(\eta,y) = A(\eta)\sin(\tau_1(y+d)) \tag{22}$$

The complete solution of (15) is given by superposition of (18) and (22). By splitting the integration interval at $y'=y$ we obtain (23) that verifies the PEC boundary condition at $y=-d$ by construction, i.e. $\tilde{E}_z(\eta,-d)=0$.
We note that for $y=0$ $\tilde{E}_z(\eta,0)=V_+(\eta)$ and

$$V_+(\eta) = -\frac{\int_{-d}^{0}\sin(\tau_1(y'+d))f_1(\eta,y')dy'}{\tau_1\cos(\tau_1 d)} + A(\eta)\sin(\tau_1 d) \tag{24}$$

By applying the Laplace transform to $H_x(x,y)$ component and considering that $\tilde{H}_{x+}(\eta,y) = -\frac{1}{j\omega\mu_o}\frac{\partial \tilde{E}_{z+}(\eta,y)}{\partial y}$ we get at $y=0$

$$\tilde{H}_{x+}(\eta,0) = I_+(\eta) = -\frac{\tau_1}{jkZ_o}A(\eta)\cos(\tau_1 d) \tag{25}$$

thus

$$A(\eta) = \frac{-jkZ_o}{\tau_1\cos(\tau_1 d)}I_+(\eta) \tag{26}$$

Substituting (26) into (25) we get the equation

$$-\frac{\int_{-d}^{0}\sin(\tau_1(y'+d))f_1(\eta,y')dy}{jkZ_o\sin(\tau_1 d)} - I_+(\eta) = Y_d(\eta)V_+(\eta) \tag{27}$$

with

$$Y_d(\eta) = -jY_c(\eta)\cot(\tau_1(\eta)d) \tag{28}$$

Eq. (27) constitutes a non-closed mathematical problem due to the presence of the integral term that depends on $f_1(\eta,y')$ (16). To render self-consistent (27) we need to explicitly represent this term using the WH unknowns of the problem. Because of the continuity of E_z and H_y at the free space-dielectric interface $x=0, -d<y<0$, we have:

$$f_1(\eta,y) = -j\eta E_z(0_-,y) + j\omega\mu_o H_y(0_-,y) \tag{29}$$

where the field inside subregion *B2* can be represented with modal expansions

$$E_z(x,y) = E_{o1}\sin\left(\frac{\pi}{d}y\right)e^{-j\chi_1 x} + \sum_{n=1}^{\infty} C_n \sin\left(\frac{n\pi}{d}y\right)e^{j\chi_n x} \tag{30}$$

since $H_y(x,y) = \frac{1}{j\omega\mu_o}\frac{\partial E_z(x,y)}{\partial x}$ and $H_x(x,y) = -\frac{1}{j\omega\mu_o}\frac{\partial E_z(x,y)}{\partial y}$. In (30) we have assumed a modal excitation of the fundamental mode according to (8), generalization is straightforward. With this representations, (29) is

$$f_1(\eta,y) = -j(\eta+\chi_1)E_{o1}\sin\left(\frac{\pi y}{d}\right) - j\sum_{n=1}^{\infty}(\eta-\chi_n)C_n\sin\left(\frac{n\pi y}{d}\right) \tag{31}$$

and the explicit expression of (27) becomes

$$\frac{-\pi(\eta+\chi_1)}{kdZ_o(\eta^2-\alpha_1^2)}E_{o1} - \sum_{n=1}^{\infty}\frac{n\pi(\eta-\chi_n)}{kdZ_o(\eta^2-\alpha_n^2)}C_n - I_+(\eta) = Y_d(\eta)V_+(\eta) \tag{32}$$

with

$$\alpha_n = \sqrt{k^2 - (\frac{n\pi}{d})^2} \tag{33}$$

that are the x-longitudinal propagation constants of the *virtual* parallel PEC plate waveguide of size d filled by free-space. Since both α_n and χ_n are located in the lower half η complex plane, the plus WH unknowns $I_+(\eta)$ and $V_+(\eta)$ are regular in $-\alpha_n$ and $-\chi_n$. Computing the residues of (32) in $\eta=-\alpha_n$ using the Cauchy Theorem and a closure of the contour in upper half η plane, it yields

$$\begin{aligned} C_1 &= \frac{E_{o1}\pi(\chi_1-\alpha_1)+2j(k^2-\alpha_1^2)V_+(-\alpha_1)}{\pi(\chi_1+\alpha_1)} \\ C_n &= \frac{+2j(k^2-\alpha_n^2)V_+(-\alpha_n)}{n\pi(\chi_n+\alpha_n)},\ n>1 \end{aligned} \tag{34}$$

By substituting (34) into (32) and by decomposing the expressions we get

$$\psi_-(\eta) + \psi_+^i(\eta) + \psi_+(\eta) - I_+(\eta) = Y_d(\eta)V_+(\eta) \tag{35}$$

where

$$\psi_+^i(\eta) = -\frac{2\pi\chi_1 E_{o1}}{dkZ_o(\eta-\alpha_1)(\alpha_1+\chi_1)} \tag{36}$$

$$\psi_+(\eta) = -j\sum_{n=1}^{\infty}\frac{(k^2-\alpha_n^2)(\alpha_n-\chi_n)}{d\alpha_n kZ_o(\eta-\alpha_n)(\alpha_n+\chi_n)}V_+(-\alpha_n) \tag{37}$$

$$\psi_-(\eta) = -j\sum_{n=1}^{\infty}\frac{(k^2-\alpha_n^2)}{d\alpha_n kZ_o(\eta+\alpha_n)}V_+(-\alpha_n) \tag{38}$$

Eq. (36) is a known source term associated to the excitation (the fundamental mode of the parallel PEC plate waveguide filled by dielectric medium), while (37) and (38) are respectively plus and minus functions that depend on the WH unknown spectrum $V_+(-\alpha_n)$ and whose singularities are the simple poles $\pm\alpha_n$ of the virtual parallel PEC plate waveguide filled by free space. Since asymptotically $\alpha_n, \chi_n = O(n)$, $(\alpha_n - \chi_n) = O(1/n)$ and $V_+(-\alpha_n), C_n = O(1/n^c)$ with $c > 1$, the convergence of the series (37) and (38) is guaranteed.

Note that (32) is an *incomplete* WH equation that models region *B* because of the unknown C_n dependence. On the contrary, (35) is a *complete* WH equation because the completeness has been guaranteed by (34) that relates the unknown C_n to the spectral WH unknown $V_+(\eta)$.

IV. Solution of the GWHEs through Fredholm factorization

The system of the GWHEs of the problem is constituted of two equations (10) and (35). The first is a GWHE were the unknowns are defined into different complex planes, while the second is a complete WH equation whose source terms depends on the knowledge of $V_+(-\alpha_n)$.

The application of Fredholm factorization [49],[10] to (10) and (35) allows to eliminate the minus unknowns $I_{a+}(-m)$ and $\psi_-(\eta)$ by contour integration. The method is based on

$$\tilde{E}_z(\eta,y)=-\frac{\int_{-d}^{y}\cos(\tau_1 y)\sin(\tau_1(y'+d))\,f_1(\eta,y')dy'+\int_{y}^{0}\cos(\tau_1 y')\sin(\tau_1(y+d))f_1(\eta,y')dy'}{\tau_1\cos(\tau_1 d)}+A(\eta)\sin(\tau_1(y+d)) \quad (23)$$

the use of Cauchy decomposition formula reported at (6). The result is to obtain integral representations that relate the plus unknowns. Their combination allows to obtain Fredholm integral equation of second kind capable to approximate the plus unknowns.

A. The Fredholm Integral Equation of the Problem

The application of Fredholm factorization to (10) with the help of (6) and (12) as reported in [25],[44],[45] yields the following integral representation that relates the plus axial spectral unknowns $V_+(\eta)$ and $I_+(\eta)$:

$$I_+(\eta)=Y_c(\eta)V_+(\eta)+\mathcal{Y}[V_+(\eta')]-I_{sca}(\eta) \quad (39)$$

for real η and η' with

$$\mathcal{Y}[...]=\frac{1}{2\pi j}\int_{-\infty}^{\infty}y(\eta,\eta')[...]d\eta \quad (40)$$

$$y(\eta,\eta')=\frac{Y_c(\eta')}{\alpha(\eta')-\alpha(\eta)}\frac{d\alpha}{d\eta'}-\frac{Y_c(\eta)}{\eta'-\eta}+\sum_{n=1}^{+\infty}\frac{q_n^{\Phi}(\eta)u(\frac{\pi}{2}-n\Phi)}{\eta'-\mathrm{p}_n^{\Phi}(\eta)} \quad (41)$$

$$p_n^{\Phi}(\eta) = \eta\cos 2n\Phi-\sqrt{k^2-\eta^2}\sin 2n\Phi \quad (42)$$

$$q_n^{\Phi}(\eta) = \frac{1}{kZ_o}(\eta\sin 2n\Phi+\sqrt{k^2-\eta^2}\cos 2n\Phi) \quad (43)$$

$$I_{sca}(\eta)=I_c(\eta)-\sum_{n=1}^{+\infty}q_n^{\Phi}(\eta)V_+^{ns}(\mathrm{p}_n^{\Phi}(\eta))u(\frac{\pi}{2}-n\Phi) \quad (44)$$

where $p_n^{\Phi}(\eta)$ and $q_n^{\Phi}(\eta)$ are related to the singularities if the kernel and $I_c(\eta)$ is the the combination of the GO source contributions due to the captured poles in Fredholm factorization procedure, see (45). In (45) we have $w_{go}=-2n\Phi+\varphi_o$, $n\in\mathbb{N}$ with corresponding GO poles $\eta_{go}=-k\cos(w_{go})$ (for instance the incident wave $\eta_o=-k\cos(-\varphi_o)$, $n=0$). $R_{ia\alpha o}$, $R_{yv\alpha}^{go}$, R_v^{go} are respectively the residues of $I_{a+}(-\alpha)$ in $\alpha(\eta_o)$, of $Y_c(\alpha)V_+(\alpha)$ in $\alpha(\eta_{go})$ and of $V_+(\eta)$ in η_{go}. Note that each w_{go} corresponds to incoming GO waves and according to the unitstep function $u()$ in (45) the number of GO waves to be considered becomes numerous when Φ is particularly small and less than $\pi/2$ (multiple reflections). In (45), the wave reflection from the subregion *B1* is taken into account with the reflection coefficient Γ_{go} (for instance the wave reflected due to the incident wave has $\Gamma_o=\frac{Y_c(\eta_o)-Y_d(\eta_o)}{Y_c(\eta_o)+Y_d(\eta_o)}$). See test case 3 of Section VI for a practical example.

Eq. (39) holds also for integration line different from the real axis but with observation points lying on the integration line [44]. We note that for $\Phi>\pi/2$ all contribution related to $p_n^{\Phi}(\eta)$ and $q_n^{\Phi}(\eta)$ disappears. These contribution are due to the fact that, while $\Phi<\pi/2$, (39) is a sectional analytic representation [68],[25], [44] due to the presence of singularity lines originated by the portion of the kernel which depends on $\alpha(\eta)$.

The application of Fredholm factorization to (35) allows to eliminate the minus unknown $\psi_-(\eta)$ by contour integration.

The method is based on the use of Cauchy decomposition formula reported at (6). We first apply contour integration of (35) along the smile contour γ_1 and we close the contour in the regularity half plane of the different integrands. We obtain that the contribution of the standard function $\psi_-(\eta)$ is null while the contributions of the standard functions $\psi_+^i(\eta)$ and $\psi_+(\eta)$ are identical to themselves.

While closing the integral in $I_+(\eta)$ we may capture non standard GO poles therefore:

$$\frac{1}{2\pi j}\int_{\gamma_1}\frac{I_+(\eta')}{\eta'-\eta}d\alpha'=I_+(\eta)-\sum_{go}\frac{R_i^{go}}{\eta-\eta_{go}}u(w_{go}+\frac{\pi}{2}) \quad (46)$$

where R_i^{go} are the residues of $I_+(\eta)$ in η_{go}.

Looking at the right end side of (35) and considering that

$$\frac{1}{2\pi j}\int_{\gamma_2}\frac{Y_d(\eta)\,V_+(\eta')}{\eta'-\eta}d\eta'=-\frac{Y_d(\eta)\sum_{go}R_v^{go}}{\eta-\eta_{go}}u(w_{go}+\frac{\pi}{2}) \quad (47)$$

$$\frac{1}{2\pi j}\int_{\gamma_1}\frac{Y_d(\eta')V_+(\eta')}{\eta'-\eta}d\eta'-\frac{1}{2\pi j}\int_{\gamma_2}\frac{Y_d(\eta)V_+(\eta')}{\eta'-\eta}d\eta'= =\frac{1}{2\pi j}\int_{-\infty}^{\infty}\frac{[Y_d(\eta')-Y_d(\eta)]V_+(\eta')}{\eta'-\eta}d\eta'+Y_d(\eta)V_+(\eta) \quad (48)$$

we obtain from (35) the integral representation

$$\psi_+^i(\eta)+\psi_+(\eta)-I_+(\eta)+I_{scd}(\eta)=Y_d(\eta)V_+(\eta)+\mathcal{Y}_d[V_+(\eta')] \quad (49)$$

where $I_{scd}(\eta)$ collects the GO source contributions due to the captured poles in Fredholm factorization procedure reported in (46) and (47) and where

$$\mathcal{Y}_d[...]=\frac{1}{2\pi j}\int_{-\infty}^{\infty}y_d(\eta,\eta')[...]d\eta \quad (50)$$

with

$$y_d(\eta,\eta')=\frac{Y_d(\eta')-Y_d(\eta)}{\eta'-\eta} \quad (51)$$

Taking inspiration from [48] and [44], the two integral representations (39) and (49), that model respectively regions *A* and *B*, can be interpreted as network relations where the current $I_+(\eta)$ is related to the voltage $V_+(\eta)$ through algebraic-integral operator admittances and short-circuit currents. These one port network models of Norton type are reported in Fig. 2 connected together in unique entire mathematical model of the problem. We note that the use of network paradigm orders and systematizes the procedure to obtain the integral representations once and for all for each kind of region as function of geometrical/material parameters.

The Fredholm integral equation (FIE) of the problem capable of approximate the spectral unknowns is obtained by eliminating $I_+(\eta)$ substituting (49) into (39) or viceversa.

The result is a FIE in terms of the unique unknown $V_+(\eta)$:

$$V_+(\eta)+\frac{1}{2\pi j}\int_{-\infty}^{\infty}M(\eta,\eta')V_+(\eta')d\eta'=N_o(\eta)+\sum_{m=1}^{\infty}h_m(\eta)V_+(-\alpha_m) \quad (52)$$

where $M(\eta,\eta')=Z_e(\eta)(\mathcal{Y}+\mathcal{Y}_d)[...]$, $Z_e(\eta)=\frac{1}{Y_c(\eta)+Y_d(\eta)}$,

$$N_o(\eta)=Z_e(\eta)(\psi_+^i(\eta)+I_{scd}(\eta)+I_{sca}(\eta)) \quad (53)$$

$$h_n(\eta)=-jZ_e(\eta)\frac{(k^2-\alpha_n^2)(\alpha_n-\chi_n)}{d\alpha_n kZ_o(\eta-\alpha_n)(\alpha_n+\chi_n)} \quad (54)$$

$$I_c(\eta) = -\frac{R_{ia\alpha o}}{\alpha(\eta)-\alpha(\eta_o)} - \sum_{go}(1+\Gamma_{go})\left(\frac{R^{go}_{yv\alpha}}{\alpha(\eta)-\alpha(\eta_{go})} - Y_c(\eta)\frac{R^{go}_{v}}{\eta-\eta_{go}}\right)u(w_{go}+\pi/2) \tag{45}$$

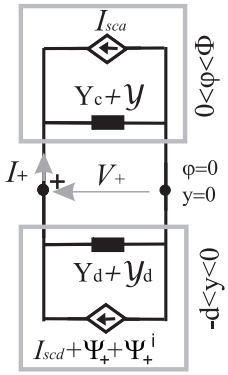

Fig. 2: Equivalent network representation of (49) into (39).

Note that (52) is a complete FIE since the source term depends on $V_+(-\alpha_m)$. In particular, we resort to the procedure reported in the Appendix of [44] inspired by [34] to demonstrate that (52) is an integral equation of Fredholm type where the kernel is compact considering a suitable generalized Hilbert space.

B. Solution of the Complete Fredholm Integral Equation

Simple numerical quadratures, such as sample and hold, allow to obtain approximate version of (52) from which we get approximate solution [50]. We note that in presence of singularities near the integration line (for instance the branch points $\pm k$ of $\tau_1(\eta)$), we need to warp the integration line on a path $v(u)$ that keeps the singularities at a suitable distance. We observe that in our problem the singularities of the kernel and of the source term are located in the 2nd and 4th quadrant (see also Figs. 13-14 of [28]), therefore we warp the real axis into the line $B_\theta : v(u) = ue^{j\theta}$, $u \in \mathbb{R}, 0 < \theta < \pi/2$ [49]. Both observation point η and integration point η' lie on B_θ to preserve the properties of the equation and avoid further contributions due to the presence of kernel singularity lines [44].

Since (52) is a FIE, to get a solution, we resort to the linearity of the equation and we apply the superposition theorem. In particular we start with the solution of:

$$V^o_+(\eta) + \frac{1}{2\pi j}\int_{-\infty}^{\infty} M(\eta,\eta')\cdot V^o_+(\eta')d\eta' = N_o(\eta) \tag{55}$$

that constitutes the equivalent physical problem where the dielectric material becomes free space, thus regions *A* and *B* are homogenous.

The sharp convergence of the kernel along B_θ allow to estimate the discretized (55) with sample and hold technique in a limited interval where A and h are respectively the truncation and the step parameters such that $A/h \in \mathbb{N}$:

$$V^o_+(v(hj)) + h\sum_{i=-A/h}^{A/h} M(v(hj),v(h\,i))V_+(v(h\,i))v'(h\,i) = N_o(v(hj)) \tag{56}$$

with $j = -A/h..A/h$. We obtain a linear system with unknowns $V^o_+(v(h\,i))$, whose solution allows to reconstruct an approximate version of $V^o_+(\eta)$ through the samples $V^o_+(v(hi))$

$$V^o_+(\eta) = -h\sum_{i=-A/h}^{A/h} M(\eta, v(h\,i))\cdot V^o_+(v(h\,i))v'(h\,i) + N_o(\eta) \tag{57}$$

As second step, we repeat the solution of (55) by changing the source term $N_o(\eta)$ with $h_n(\eta)$ $n \in \mathbb{N}$. The discretized solution labeled $V^n_+(v(hi))$ allows to reconstruct $V^n_+(\eta)$ as done for $V^o_+(\eta)$.

By means of superposition, an implicit solution of the original problem (52) is

$$V_+(\eta) = V^o_+(\eta) + \sum_{m=1}^{\infty} V^m_+(\eta)V_+(-\alpha_m) \tag{58}$$

in terms of the unknown coefficients $V_+(-\alpha_m)$.

By enforcing

$$V_+(-\alpha_n) = V^o_+(-\alpha_n) + \sum_{m=1}^{\infty} V^m_+(-\alpha_n)V_+(-\alpha_m) \tag{59}$$

we obtain an approximation of coefficients $V_+(-\alpha_m)$. Since the system (59) is of infinite dimensions we limit the $n = m$ terms to a maximum value M by considering the cut-off of the *virtual* parallel PEC plate waveguide of size d (subregion *B1*). Once the first M coefficients are known, (58) becomes an approximate explicit representation of $V_+(\eta)$. Convergence of (59) is guaranteed by the properties reported in Section III-B. Practical details on the selection of M are reported in Section VI.

V. Evaluation of Electromagnetic Field

For the presence of multi-variate functions depending on $\tau_1(\eta)$ (with proper and improper sheets) and of sectional analytic functions (when $\Phi < \pi/2$), the approximate axial spectrum of $V_+(\eta)$ directly obtained from the discretization of (52) via (58) is valid only in a limited portion of η complex plane that is not sufficient to compute the fields via inverse Laplace transform and asymptotics. In particular to get an extended validity in the proper sheet of η plane when $\Phi < \pi/2$ we need to consider extra singularity lines while the observation point η is out of the integration line used to solve the FIE, see [44] for details. Once obtained the approximated spectrum of $I_+(\eta)$ via discretized versions of (10) and (35) in terms of $V_+(\eta)$ in the proper sheet of the η complex plane, we perform analytic continuation of the approximated spectrum (see Appendix) by resorting to recursive equations in w directly obtained from the system of GWHEs (10) and (35) after some mathematical manipulations (see Appendix A). The w complex plane is defined by the mapping $\eta = -k\cos w$ that is reported for example in [28] with its properties and its connection to η complex plane. In particular in this plane we define the quantities $\hat{V}_+(w) = V_+(-k\cos w)$ and $\hat{I}_+(w) = I_+(-k\cos w)$ (the axial spectra in w), i.e. the Laplace transforms in the w plane of the electromagnetic field at $\varphi = 0$.

In the following we consider two kind of sources: i) a E_z plane wave incident from the angular region *A* and/or ii) the TE_n x-progressive mode from the parallel PEC plate waveguide filled by dielectric of subregion *B2*.

In region *A* we are interested on the computation of far-field components (GO/UTD), while in subregion *B1* the interest is focused on TE_n x-regressive modal field excited by the sources. We recall that all the physical singularities of fields are explicitly contained in the semi-analytical expression of the approximated spectrum.

For what concerns region *A*, given the axial spectra, the theory of rotating waves [69] allows to obtain the spectra $V_+(\sigma,\varphi)$, $I_+(\sigma,\varphi)$ for any azimuthal direction φ in w plane. In particular we obtain for $\hat{V}_d(w,\varphi)=\sin(w)\hat{V}_+(w,\varphi)$ and $\hat{I}_+(w,\varphi)$:

$$\begin{cases} \hat{V}_d(w,\varphi) = \frac{Z_0(\hat{I}_+(w-\varphi)-\hat{I}_+(w+\varphi))+\hat{V}_d(w-\varphi)+\hat{V}_d(w+\varphi)}{2} \\ \hat{I}_+(w,\varphi) = \frac{Z_0(\hat{I}_+(w-\varphi)+\hat{I}_+(w+\varphi))+\hat{V}_d(w-\varphi)-\hat{V}_d(w+\varphi)}{2Z_0} \end{cases} \tag{60}$$

in terms of $\hat{V}_d(w=\sin(w)\hat{V}_+(w)$ and $\hat{I}_+(w)$ for $0\le\varphi\le\Phi$.

By applying the inverse Laplace transform in w plane to $\hat{V}_+(w,\varphi)$ we obtain

$$E_z(\rho,\varphi)=\frac{k}{2\pi}\int_{\lambda(B_r)}\hat{V}_+(w,\varphi)e^{jk\rho\cos w}\sin w dw \tag{61}$$

where $\lambda(B_r)$ is the Bromwich contour B_r of η plane mapped into w plane, see for details [69]. Similar considerations holds for $H_\rho(\rho,\varphi)$ field component that is obtained from $\hat{I}_+(w,\varphi)$.

The application of the residue theorem and of the steepest descent path (SDP) method provide the evaluation of far-field GO/UTD components (see an application in [43]):

$$E_z(\rho,\varphi)=E_z^g(\rho,\varphi)+E_z^d(\rho,\varphi) \tag{62}$$

where the contributions of poles captured by contour deformation/closure give GO components $E_z^g(\rho,\varphi)$ and the integral along the SDP is the diffracted component $E_z^d(\rho,\varphi)$:

$$E_z^g(\rho,\varphi)=-jk\sum_i \mathrm{Res}[\hat{\mathrm{V}}_\mathrm{d}(\mathrm{w},\varphi)]_{\mathrm{w_i}(\varphi)}\ \mathrm{e}^{+\mathrm{jk}\rho\cos\mathrm{w_i}(\varphi)} \tag{63}$$

$$E_z^d(\rho,\varphi)=-\frac{ke^{-jk\rho}}{2\pi}\int_{\mathrm{SDP}}\hat{V}_d(w,\varphi)e^{k\rho h(w)}dw \tag{64}$$

with $h(w)=k\rho(\cos w+1)$, $w_i(\varphi)=w_{oi}\pm\varphi$ and w_{oi} are the GO poles of the axial spectrum $\hat{V}_d(w)$.

Approximating $E_z^d(\rho,\varphi)$ with the saddle point at far distance $k\rho>>1$, we obtain the GTD component of the field:

$$E_z^{gtd}(\rho,\varphi)=E_o\frac{e^{-j(k\rho+\frac{\pi}{4})}}{\sqrt{2\pi k\rho}}D(\varphi) \tag{65}$$

$$D(\varphi)=\frac{-k\hat{V}_d(-\pi,\varphi)}{jE_o} \tag{66}$$

This expression clarifies the importance of the recursive equations of the Appendix A. In fact, to estimate $\hat{V}_d(-\pi,\varphi)$ in $0<\varphi<\Phi$, we need the axial spectra defined in the range $-\pi-\Phi<w<-\pi+\Phi$ and usually the initial approximated spectra is a portion of proper sheet of η plane i.e. a portion of w plane that does not contain $-\pi<w<0$, see Appendix I of [28].

With plane wave source, we have shadow boundaries of GO components (related to the poles $w_i(\varphi)=w_{oi}\pm\varphi$ that crosses the SDP). In this case, to compensate the caustics of GTD component we apply the Uniform Theory of Diffraction (UTD) [70] to get uniform fields:

$$E_z^{utd}(\rho,\varphi)=E_o\frac{e^{-j\left(k\rho+\frac{\pi}{4}\right)}}{\sqrt{2\pi k\rho}}C(\varphi,\varphi_o) \tag{67}$$

$$C(\varphi,\varphi_o)=D(\varphi)+\sum_q\Gamma_q\frac{1-F\left(2k\rho\cos^2\frac{\varphi-\varphi_q-\pi}{2}\right)}{\cos\frac{\varphi-\varphi_q-\pi}{2}} \tag{68}$$

where Γ_q are the coefficients of the GO components with outward direction φ_q and the function $F(z)$ is the Kouyoumjian-Pathak transition function defined in [70] and its application in the framework of WH technique is reported in (63) of [28].

In case of source constituted of modal field, the diffracted component does not need uniformization because of the absence of shadow boundaries/caustics.

Finally, the estimation of the intensity of the TE_n x-regressive modal field in region *B1* excited by the sources is obtained straightforward from (30) computing C_n (34).

VI. Validation and Numerical Results

With reference to the problem described in Fig. 1 at E_z polarization, we provide validations and numerical results of the proposed method in relation to the geometrical and physical parameter of the problem (d, Φ, ε_r) and the sources: 1) incident plane wave source characterized by (7) with intensity $E_{go}=E_o=1V/m$ and incoming direction $\varphi_{go}=\varphi_o$, 2) modal excitation via TE_n x-progressive modal field (8).

The solution of (52) via (58) reported in the following subsections are obtained via semi-analytical procedure with discretization parameters A,h (see Section IV-B).

In the following test cases we make self-convergence tests and validation thorough an independent fully numerical solution obtained by a in-house code based on the Finite Element Method (FEM) embedding singular modelling [64]-[66] with the following setup: region truncated at a distance of $\rho=10\lambda$ from the origin O with perfectly matched layer of cylindrical shape of depth $\lambda/2$ and quadratic triangular elements with max side length of $\lambda/10$.

In the following, we consider all the angles in radians by omitting rad. For computational purpose, we have selected $k=k_r-jk_i$ with $k_r=1$. The analysis of problem for practical values of geometrical/electromagnetic parameters is obtainable by scaling the quantities according to [42]: a different value of k_r, e.g. $k_r=p$, changes the resulting axial spectra $\{V_+(\eta),I_+(\eta)\}$ to $\left\{\frac{1}{k}V_+(\frac{\eta}{k}),\frac{1}{k}I_+(\frac{\eta}{k})\right\}$.

A. Test Case 1

In the first test case we analyze the convergence, the self-convergence and the validation of the proposed method for the analysis of the structure presented in Fig. 1 with an E_z plane wave illumination. The solution and its convergence is studied in terms of spectral quantities, diffraction coefficients, total far fields in region *A* and modal fields excited in subregion *B2*.

In this test case we consider the following physical parameters: $E_o = 1V/m$ and $k = k_r - jk_i$ with $k_i = 0.0001k_r$ ($k_r = 1$), $\varphi_o = 0.3\pi$, $d = 0.55\lambda$, $\Phi_a = 0.8\pi$, $\varepsilon_r = 2$.

According to GO, the E_z-polarized incident plane wave impinges on the structure and generates an outgoing reflected wave from the PEC face $\varphi = \Phi$ ($\varphi_{RA} = -\pi + 2\Phi_a - \varphi_o = 0.3\pi$) and an outgoing reflected wave from the layer $x > 0, y = 0$ subregion *B1* ($\varphi_{RD} = \pi - \varphi_o = 0.7\pi$). We note that the directions of the waves identify also the shadow boundaries. Moreover, the source excites modal fields in subregion *B2*, where only the first TE_n ($n = 1$) mode is above cut-off, since $k_r\sqrt{\varepsilon_r}d/\pi \simeq 1.56$, see (9).

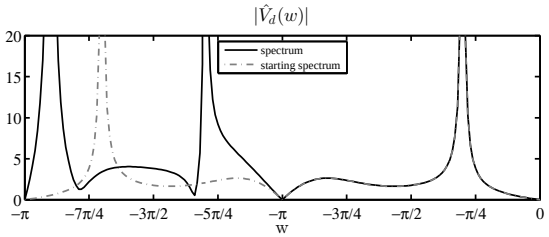

Fig. 3: Test case 1: absolute value of the approximated spectrum $\hat{V}_d(w)$ obtained for $A = 50, h = 0.05, M = 3$ (reference solution) before and after the application of recursive equations respectively labeled starting spectrum and spectrum.

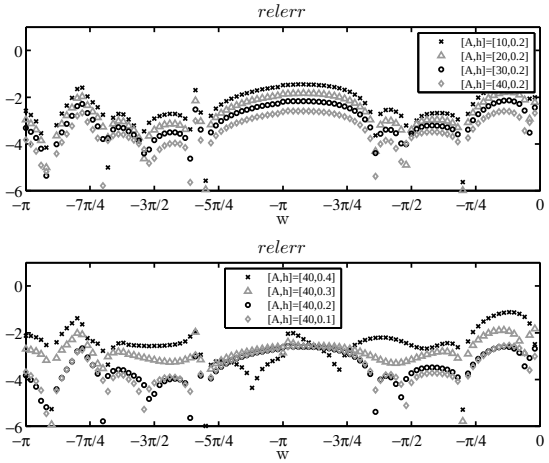

Fig. 4: Test case 1: self-convergence test of $\hat{V}_d(w)$ for various values of integration parameters A (top) and h (bottom). The relative error with respect to the reference solution is computed in $\log_{10}$ scale.

The full convergence of the solution of the problem is obtained applying the discretization method reported in Section IV-B to (52) via (58).

With the physical parameters reported in this test case, we note that the source (53) in the FIE (52) is only constituted of some of the terms: we neglect ψ^i due to the absence of modal excitation and we need to consider contributions only of the first reflections from the PEC face $\varphi = \Phi$ and the subregion *B1*. Due to the geometrical parameters of the problem, no singularity lines is present [44] since $\Phi > \pi/2$. In practice, in $I_c(\eta)$ of $I_{scd}(\eta)$ (45) and, in (46) and (47) of $I_{scd}(\eta)$ we consider only the terms due to the incident plus the *B1* reflected waves with $w_o \equiv w_{RD} = -\varphi_o = -0.3\pi = -\pi + \varphi_{RD}$ and

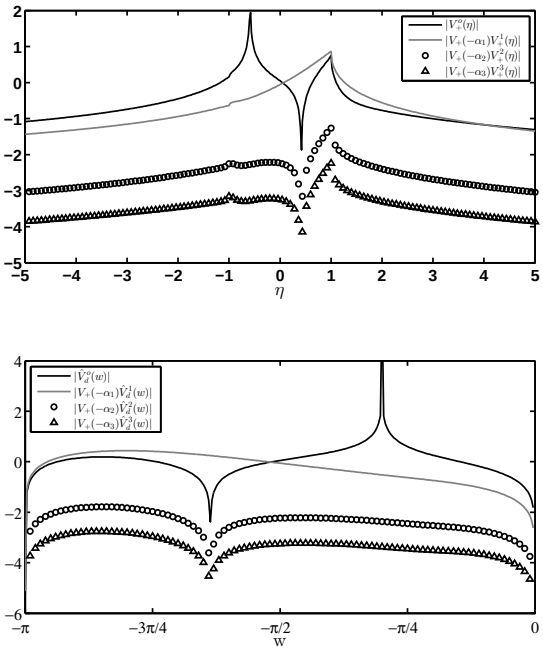

Fig. 5: Test case 1: on top $|V_+^o(\eta)|$ and $|V_+(-\alpha_m)V_+^m(\eta)|$ in $\log_{10}$ scale for $-5 < \eta < 5$, on bottom $|\hat{V}_d^o(w)|$ and $|V_+(-\alpha_m)\hat{V}_d^m(w)|$ in $\log_{10}$ scale for $-\pi < w < 0$, where $\hat{V}_d^o(w) = \sin w V_+^o(-k\cos w)$ and $\hat{V}_d^m(w) = \sin w V_+^m(-k\cos w)$. $V_+(-\alpha_m) = [4.099 + 1.471j, 0.363 - 0.030j, 0.165 - 0.0227j]$. Results for $A = 50, h = 0.05, M = 3$ (reference solution).

we neglect the term related to the face $\varphi = \Phi$ reflected wave with $w_{RA} = -2\Phi_a + \varphi_o = -1.3\pi = -\pi - \varphi_{RA}$.

First we discuss the solution, step by step. We consider as reference solution the one obtained from the discretization of (52) with integration parameters $A = 50, h = 0.05$ in terms of $V_+(\eta)$. To get an explicit solution we consider the procedure proposed in subsection IV-B by considering the first three h_m terms that correspond to the first three TE_n modes of the dielectric-loaded parallel PEC plate waveguide with size d (see $M = 3$ in Section IV-B). We note that since $k_r\sqrt{(\varepsilon_r)}d/\pi \simeq 1.56$ see (9) and $k_r d/\pi = 1.1$ see (33), only the first mode is above cut-off, thus two extra evanescent modes are used to correctly match the field at the free-space/dielectric interface $x = 0$, $-d < y < 0$.

In Fig.3 we show the spectrum in w plane of $V_+(\eta)$ before and after the application of the recursive equations reported in the Appendix. As expected the singularities of GO field are correctly determined in the extended spectrum in w plane at w_o and w_{RA}, and their residues are used to compute the GO component in (63).

Fig.4 demonstrates the self-convergence of the absolute value of $\hat{V}_d(w)$ for $A \gtrsim 40$ and $h \lesssim 0.2$, by obtaining spectral approximation of $\hat{V}_d(w)$ with relative error less than 10^{-3}.

Fig.5 highlights the contribution of h_m terms in the total spectrum of $\hat{V}_d(w)$ in terms of $V_+^o(\eta)$ and $V_+(-\alpha_m)V_+^m(\eta)$ according to (58). As shown the relevant contributions are given by the first term as $m = 1$ is dominant with respect to the successive terms $m = 2, 3$.

In Tables I, II, III we focus the attention on the convergence of modal fields excited inside the dielectric-loaded parallel

PEC plate waveguide (subregion *B2*) that influences the quality of the global solution of the problem, see (52). Table I reports the exact TE_n modal propagation constant χ_n normalized by k and the computed coefficients C_n (34) of the x-regressive TE_n modes for the reference solution. Although C_n (34) are in general very sensitive to errors or lack in precision, Tables II and III demonstrate the convergence of the computed C_n for $A \gtrsim 40$ and $h \lesssim 0.2$ ($M = 3$). Moreover, we note that between the first and the fifth mode we have a scale factor of $\backsim 75$ in terms of absolute values:

$$|C_1/C_n| = [1., 10.6, 28.5, 50.0, 74.6] \tag{69}$$

TABLE I: Modal expansion for $A = 50, h = 0.05, M = 3$

TE_n	χ_n/k	C_n
1	1.0833 + 0.0001j	0.5053 - 1.4490j
2	0.0003 + 1.1427j	0.1440 - 0.0096j
3	0.0003 + 2.3320j	0.0536 - 0.0060j
4	0.0004 + 3.3501j	0.0304 - 0.0045j
5	0.0005 + 4.3199j	0.0202 - 0.0036j

TABLE II: Relative error of C_n for $h = 0.2$

TE_n	$A = 10$	$A = 20$	$A = 30$	$A = 40$
1	0.0046	0.0022	0.0011	0.0005
2	0.0368	0.0175	0.0085	0.0034
3	0.0624	0.0303	0.0149	0.0059
4	0.0832	0.0415	0.0206	0.0082
5	0.1001	0.0511	0.0256	0.0103

TABLE III: Relative error of C_n for $A = 40$

TE_n	$h = 0.4$	$h = 0.3$	$h = 0.2$	$h = 0.1$
1	0.0114	0.0023	0.0005	0.0004
2	0.0058	0.0033	0.0034	0.0034
3	0.0076	0.0054	0.0059	0.0059
4	0.0093	0.0073	0.0082	0.0082
5	0.0108	0.0090	0.0103	0.0102

We note that the expression of C_n (34) depends on the spectrum $V_+(\eta)$ computed in the regular half-plane, far from its singularities, therefore quite-regular. For this reason, although we have considered only three h_m terms ($M = 3$) we get precise estimation of C_n for n grater than 3. In order to analyze the effect of modal expansion in (52) via (58) and the relevance of the numbers of the considered modes, Fig. 6 reports the intensity of the first three TE_n modes and the total field combining the first five modes at $x = 0$, $-d < y < 0$. As expected the fundamental mode, which propagates, and the second mode, which is an evanescent mode, are the dominant contributions. The convergence is also studied in terms of GTD diffraction coefficient (66), see Fig. 7, where on the top of the figure the absolute value is reported in dB scale versus the observation angle φ. The peaks of the GTD diffraction coefficients occur for the GO angles: the outgoing reflected waves $\varphi_{RA} = 0.3\pi$ and $\varphi_{RD} = 0.7\pi$. On the bottom of Fig. 7 the convergence is shown for different integration parameters through the evaluation of the relative error in log_{10} scale with respect to the reference solution. This scale measures the precision in term of digits.

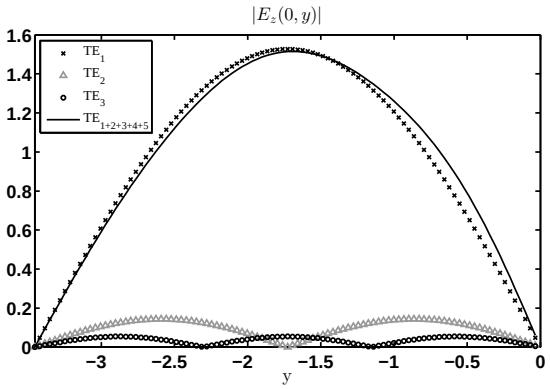

Fig. 6: Test case 1: absolute value of $E_z(0, y)$ of the first three TE_n modes and of the total field combining the first five modes at $x = 0$, $-d < y < 0$. Results are obtained for integration parameters $A = 50, h = 0.05, M = 3$ in (52) via (58) (reference solution).

With reference to Fig. 1, the absolute value of total far field (62) in region *A* at a distance of $k_r\rho = 10$ from O is reported in Fig. 8 the reference solution $A = 50, h = 0.05$ with three h_m terms, also in terms of GO field component (63) and UTD field component (67). The figure reports also the comparison between the reference solutions and the solution obtained with same parameters but with the subregion *B1* filled by free-space. The mathematical interpretation of this last solution is equivalent to ignore mode expansion at the free-space/dielectric interface, since all h_m terms are null ($\alpha_m = \chi_m$, i.e. $M = 0$). We note that the diffracted component is significantly sensitive to the presence of the dielectric and also depends on the inclusion of h_m terms.

Finally Fig. 9 shows an independent validation by comparing the results obtained for the reference solution and application of FEM code as described previously in the introduction of Section VI in terms of absolute value and phase of the total far field. We recall that the phase is a very sensitive parameter to check the quality of convergence in comparison to the absolute value. The agreement between the two solutions is evident, in particular we notice that to capture the sharp behaviour of the phase in the region $\pi/4 < \varphi < \pi/3$ we have fully studied the convergence of our method and FEM. In fact both methods are very sensitive to this physical behavior, therefore the inclusions of several modes (three h_m terms) in our technique and the refinement of FEM solution have been necessary.

B. Test Case 2

The second test case illustrates the solution while the source is constituted of the first TE_n mode that propagates in the dielectric-loaded parallel PEC plate waveguide with size d (subregion *B2*). The geometrical and physical parameters of the problem are the same as reported in test case 1. The intensity of the TE_1 source is $E_{o1} = 1V/m$ (8). As in test case 1 only the first TE_n ($n = 1$) mode is above cut-off, since $k_r\sqrt{\varepsilon_r}d/\pi \simeq 1.56$, see (9).

The solution of (52) via (58) shows performances on convergence similar to test case 1, thus in this test we focus the

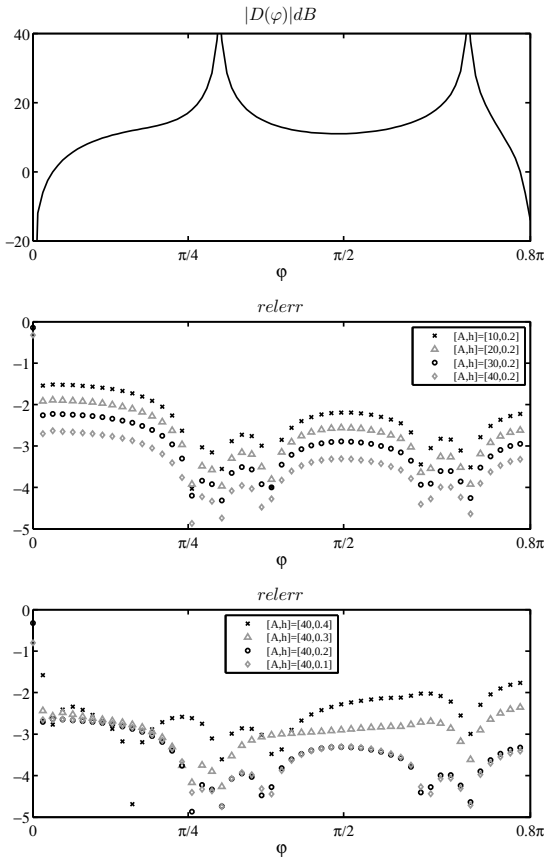

Fig. 7: Test case 1: on top the absolute value of GTD diffraction coefficient is reported in dB, on center and bottom the relative error on the computation of GTD diffraction coefficient in log_{10} scale for different integration parameters A, h with respect to the reference solution $A = 50, h = 0.05$ ($M = 3$). The peaks of the GTD diffraction coefficients occur for the GO angles $\varphi_{RA} = 0.3\pi$ and $\varphi_{RD} = 0.7\pi$.

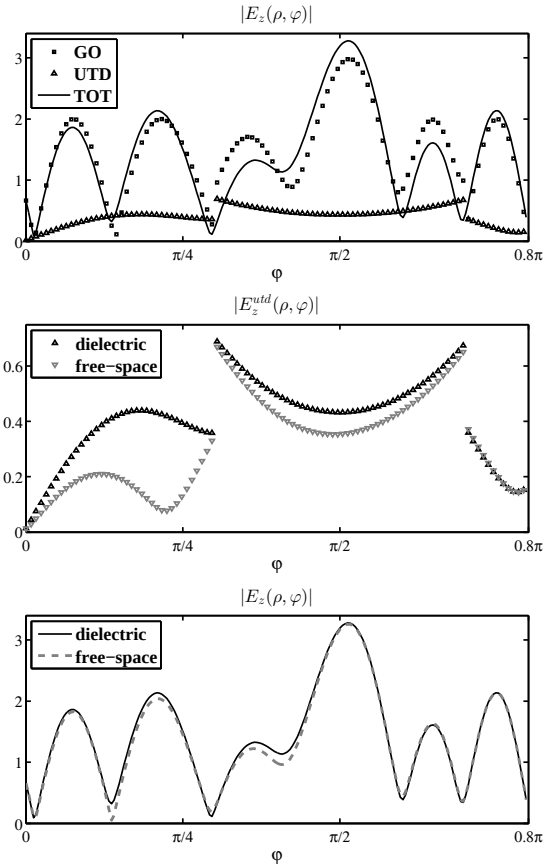

Fig. 8: Test case 1: on top the GO field, the UTD component and, the total far-field pattern at $k_r\rho = 10$ for the reference solution $A = 50, h = 0.05$ with three h_m terms ($M = 3$), on center and bottom respectively the UTD component and, the total far-field pattern at $k_r\rho = 10$ for the reference solution and the solution obtained with same parameters but with the subregion *B1* filled by free-space ($M = 0$).

attention on the different physics phenomena of the problem for the reference solution obtained with $A = 40, h = 0.1$ and three h_m terms ($M = 3$).

In region *A* no GO field is present, thus the total far field is constituted of the GTD component without shadow boundary. In subregion *B2*, the source excites x-regressive modal fields with higher intensity with respect to test case 1, as expected. In this test case, the FIE's source (53) is constituted only of ψ^i term due to the the modal excitation while I_{sca} and I_{scd} are null.

Without loss of clarity, we do not report the spectrum in w of $V_+(\eta)$, that in this case is continuous without peaks. The application of saddle point technique allows to obtain the total far field component (65) in region *A* at a distance of $k_r\rho = 10$ from O (Fig. 1) in terms of GTD diffraction coefficient (66), see Fig. 10 on top where the comparison between dielectric and free space filling of subregion *B2* is reported. We recall that in case of free space filling of subregion *B2* all h_m terms are null in (52). On the bottom of Fig. 10 the convergence is shown for different integration parameters through the evaluation of the relative error in log_{10} scale with respect to the reference solution obtained for $A = 40, h = 0.1, M = 3$.

In order to analyze the effect of excited TE_n modes, Fig. 11 reports the intensity of electric field of modal expansions at $x = 0$, $-d < y < 0$. Since only the fundamental TE_1 mode propagates and due to the kind of excitation (TE_1 mode), we have that C_n have higher values and decrease slowly in comparison with test case 1. In fact we have that the first 12 values are greater than $|C_1|/75$

$$|C_1/C_n| = [1., 3.7, 8.6, 13.9, 19.8, 26.1, 32.8, 39.9, 47.5, 55.3, 63.4, 71.9, 80.6, 89.7, 98.9, 108.4, 118.2, 128.2] \quad (70)$$

Similar convergence properties are obtained while subregion *B2* is filled by free-space. As reported in Fig. 11 the most relevant contribution comes from C_1 in both cases. In particular we not that for dielectric filling of subregion *B2* $(E_{o1} + C_1)/E_{o1} = 1.325 + 0.166j$ while for free space $(E_{o1} + C_1)/E_{o1} = 0.846 + 0.180j$ due to the reflection properties at the port $x = 0, -d < y < 0$ and phase composition.

C. Test Case 3

This test case illustrates the solution for a practical example where: $k = k_r - jk_i$ with $k_i = 0.0001k_r$ ($k_r = 1$), $d =$

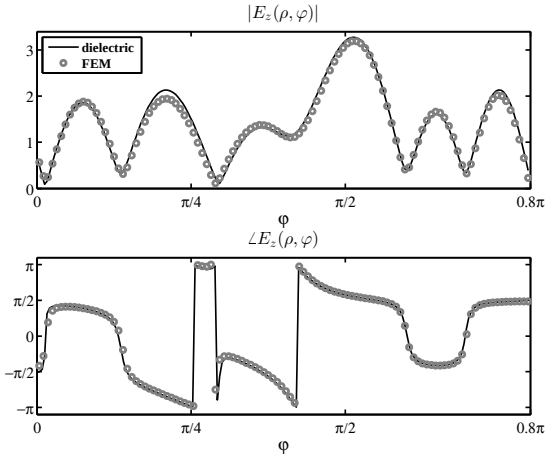

Fig. 9: Test case 1: absolute value (top) and phase (bottom) of the total far-field pattern at $k_r\rho = 10$ for the reference solution $A = 50, h = 0.05$ with three h_m terms compared with the same quantity obtained thought FEM code as described in the introduction of Section VI.

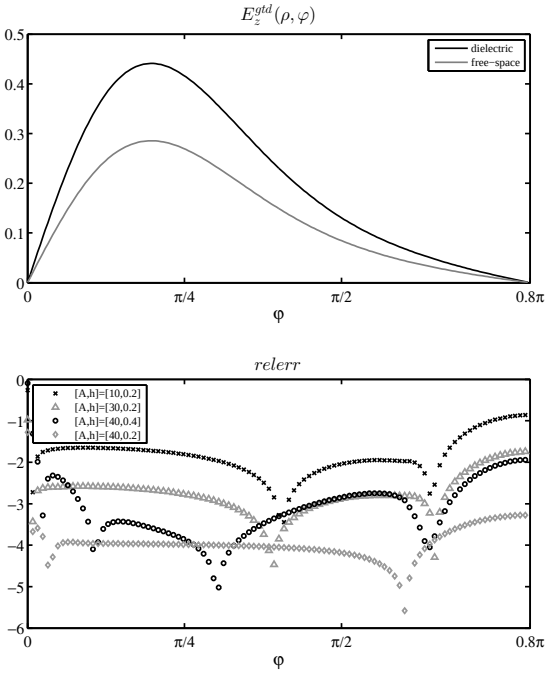

Fig. 10: Test case 2: on top the absolute value of total far field (65) in region *A* at a distance of $k_r\rho = 10$ from *O* (Fig. 1), on bottom the relative error in log_{10} scale for different integration parameters A, h with respect to the reference solution $A = 40, h = 0.1, M = 3$.

1.10λ, $\Phi_a = 50\pi/180$ (50^o), $\varepsilon_r = 5$ with an illumination constituted of a E_z-polarized incident plane wave with $\varphi_o = 45\pi/180$ and $E_o = 1V/m$. In this test case we stress our methodology by considering acute aperture angle of region *A* that generates multiple reflections, denser dielectric and multi-modal propagation in subregions *B2*.

According to [44], while the angular region is acute we need to consider singularity lines contribution, see also Section IV, V for discussion. In this case we need to consider p_1^Φ to get the solution in terms of starting spectra and then we need to consider also p_2^Φ to extend the validity of spectra in w plane

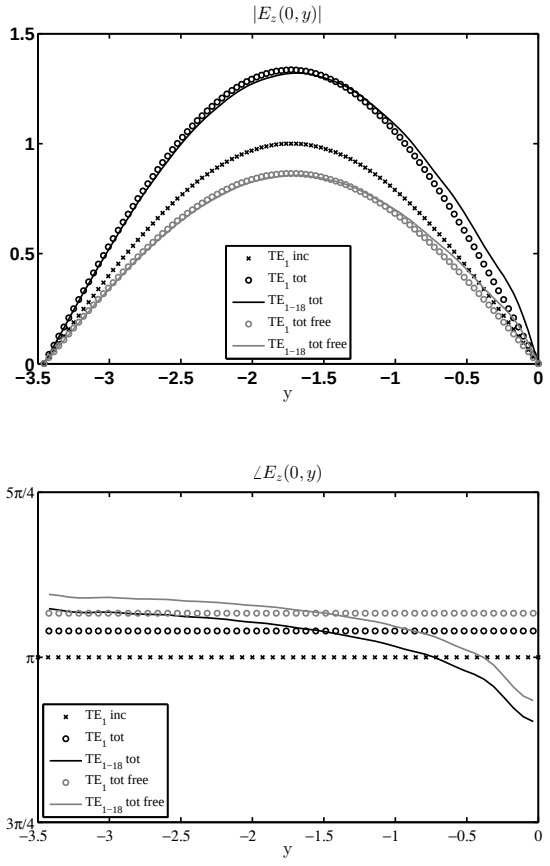

Fig. 11: Test case 2. On top absolute value of $E_z(x,y)$ at $x = 0$, $-d < y < 0$ for the incident TE_1 mode, the total electric field combining the incident and reflected TE_1 mode and for the total field combining the incident TE_1 and the first 18 reflected TE_n modes respectively while subregion *B2* is filled by dielectric medium (black) and by free-space (gray). On bottom the same results for the phase of the total electric field. The numerical results are reported for the reference solution with $A = 40, h = 0.1, M = 3$.

for $w < w_{p_2^\Phi} - 4\Phi + \pi/2 = -1.920$ to contain the interval $-\pi < w < 0$ [44] needed for the application of recursive equations (Appendix A).

Since $k_r\sqrt{\varepsilon_r}d/\pi \simeq 4.919$ the first four TE_n modes are above cut-off. For this reason we select as reference solution of (52) via (58) the one obtained with $A = 40, h = 0.1$ and five h_m terms ($M = 5$). According to GO, the E_z-polarized incident plane wave (with incoming direction φ_o and outgoing direction $\varphi_I = -\pi + \varphi_o$) impinges on the structure and generates further 7 waves: 1) starting with the first reflection from the PEC face $\varphi = \Phi$

$$[\varphi_{RA}, \varphi_{RCRA}, \varphi_{RARCRA}, \varphi_{RCRARCRA}] = [-\pi + 2\Phi - \varphi_o, \pi - 2\Phi + \varphi_o, -\pi + 4\Phi - \varphi_o, \pi - 4\Phi + \varphi_o] \tag{71}$$

2) starting with the first reflection from the subregion *B1*

$$[\varphi_{RC}, \varphi_{RARC}, \varphi_{RCRARC}] = \\ = [\pi - \varphi_o, -\pi + 2\Phi + \varphi_o, \pi - 2\Phi - \varphi_o] \tag{72}$$

Poles in η plane are obtained with $\eta_{go} = -k\cos w_{go}$ with $w_{go} = -2\Phi + \varphi_o, -2\Phi + \varphi_o, -4\Phi + \varphi_o, -4\Phi + \varphi_o$ corresponding to waves first reflected from the PEC face $\varphi = \Phi$ (case 1) and with $w_{go} = -2\Phi - \varphi_o, -2\Phi - \varphi_o, -4\Phi - \varphi_o$

corresponding to waves first reflected from subregion *B1* (case 2). The reflection coefficient from the PEC face $\varphi = \Phi$ is -1 while the reflection coefficient from the subregion *B1* is given by

$$\Gamma_{go} = \frac{Y_c(\eta_{go}) - Y_d(\eta_{go})}{Y_c(\eta_{go}) + Y_d(\eta_{go})} \tag{73}$$

where $Y_c(\eta)$ and $Y_d(\eta)$ are defined in Section III.

For what concerns the GO component we note that only the last reflections $\varphi_{RCRARCRA}$, φ_{RCRARC} generate shadow boundaries.

With the physical parameters reported in this test case, we note that the FIE's source (53) is only constituted of some of the terms: we neglect ψ^i due to the absence of modal excitation and we need to consider the GO contributions of φ_I, φ_{RA}, φ_{RC} and φ_{RCRA} waves in $I_c(\eta)$ (45) of $I_{sca}(\eta)$ (44) and in $I_{scd}(\eta)$ (47). Due to the acute aperture angle Φ, p_1^Φ needs to be considered in (44).

First we discuss the solution in terms of the spectrum $\hat{V}_d(w)$: Fig. 12 shows on top the effect the inclusion p_2^Φ on the approximate solution while extending the spectrum toward $w = -\pi$ from $w = 0$, on bottom the figures shows the spectrum $\hat{V}_d(w)$ extended by recursive equations up to $w = -2\pi$.

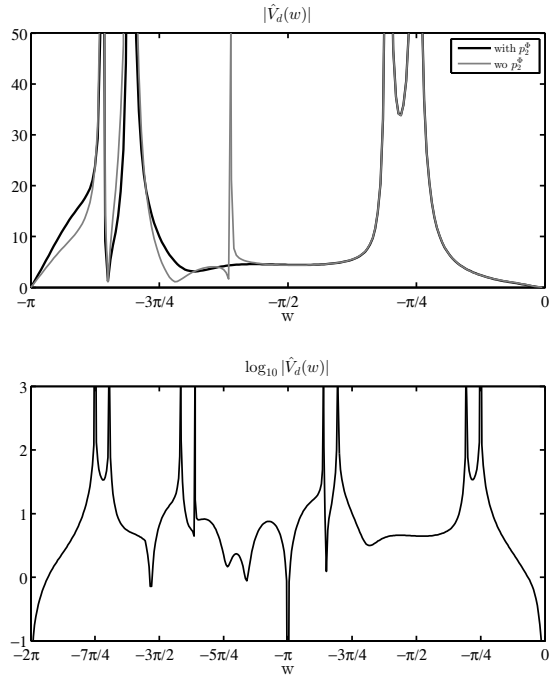

Fig. 12: Test case 3. On top $|\hat{V}_d(w)|$ with or without considering p_2^Φ for $-\pi < w < 0$: we notice the spike at $w_{p_2^\Phi} = -4\Phi + \pi/2$ corresponding to p_2^Φ and GO peaks at $w_o = -\varphi_o$ and $w_{ra} = -2\Phi + \varphi_o$. On bottom $\log_{10}|\hat{V}_d(w)|$ with p_2^Φ and after the application of recursive equations: we notice the GO peaks at $w_{go} = \pm\varphi_o - 2n\Phi$ with $n \in \mathbb{N}$. Results for $A = 40, h = 0.1, M = 5$.

With reference to Fig. 1, the absolute value of total far field (62) in region *A* at a distance of $k_r\rho = 10$ from O is reported in Fig. 13 for the reference solution $A = 40, h = 0.1, M = 5$, also in terms of GO (63) and UTD (67) field components.

In order to analyze the effect of excited TE_n modes in subregion *B2*, Fig. 14 reports the intensity of electric field as

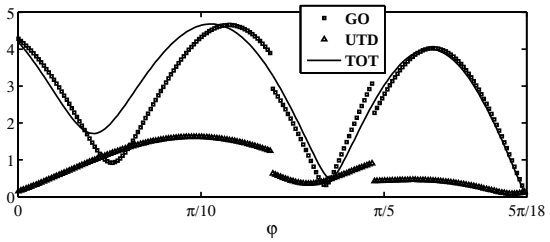

Fig. 13: Test case 3: GO field, the UTD component and, the total far-field pattern at $k_r\rho = 10$ for the reference solution $A = 40, h = 0.1, M = 5$. Shadow boundaries are at $\varphi_{RCRARCRA}$, φ_{RCRARC}.

modal expansions at different value of x and for a different number of modes. In this test case, due to the geometry and materials, we have that: 1) the most intense C_n is the second one ($|C_2|$ is twice of $|C_1|$ and $|C_3|$), 2) C_n decrease slowly with respect to the previous test cases, 3) only the first four modes are propagating. These considerations are summarizes in Table IV and shown in Fig. 14.

TABLE IV: Modal expansion for $A = 10, h = 0.1, M = 5$

TE_n	χ_n/k	C_n
1	2.18938 - 9 10^{-6}j	-0.32391 + 0.03023j
2	2.04293 - 0.00004j	-0.38061 - 0.59211j
3	1.77214 - 0.00010j	-0.16863 - 0.24266 j
4	1.30162 - 0.00025j	-0.048750 - 0.17580j
5	0.00127 - 0.40656j	0.04277 - 0.09959 j
6	0.00048 - 1.56141j	0.01876 - 0.04745j
7	0.00045 - 2.26362j	0.01120 - 0.03080j
8	0.00046 - 2.86760j	0.00738 - 0.02208j
9	0.00049 - 3.42572j	0.00515 - 0.01679j
10	0.00052 - 3.95742j	0.00374 - 0.01328j

VII. Conclusions

This paper demonstrates the effectiveness of the quasi-analytical method known as GWHT in studying radiation and scattering complex canonical problems. In particular in this paper we have examined an arbitrarily flanged dielectric-loaded waveguide that resembles scattering analysis for example in radar applications such as inlets in aerospace engineering or antenna problem similar to a horn fed by a waveguide loaded by a dielectric material. In this problem the GWHT is further extended and it is now capable of handling piecewise constant inhomogeneous dielectric layers by resorting to the application of characteristic Green's function procedure starting from the wave equation.

The problem is formulated in a unique entire model based on GWHEs with the help of network interpretations that takes into consideration the true near-field interaction among the different materials and structures.

The numerical results shows the efficacy of the method. he semi-analyticity of the GWHT solution allows engineering and physical insights in terms of spectral component of electromagnetic field, GTD/UTD diffraction coefficients, total far fields and modal fields.

In this paper we have used a novel and effective procedure to handle with complete WH equations, GWHEs via FIEs that is described in Sections III and IV.

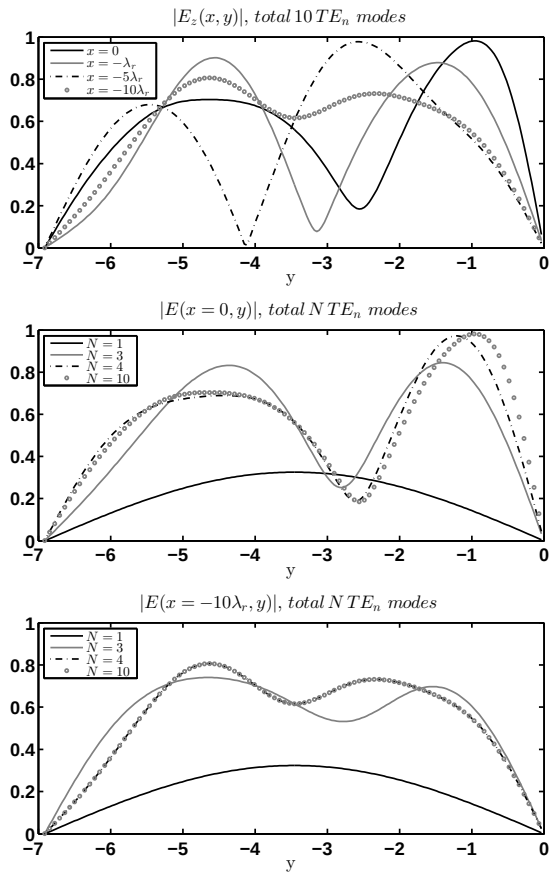

Fig. 14: Test case 3. On Top the intensity of electric field obtained considering the first 10 modes is plotted for different values of $x = 0, -\lambda_r, -5\lambda_r, -10\lambda_r$. The intensity of electric field obtained considering the first N modes is plotted for $x = 0$ (center) and $x = -10\lambda_r$ (bottom). Results for $A = 40, h = 0.1, M = 5$.

APPENDIX A
ANALYTIC CONTINUATION

To analytically extend the validity of the approximated spectra $V_+(\eta)$ and $I_+(\eta)$ in roper and improper sheets we resort to recursive equations in w plane ($\eta = -k\cos w$) directly obtained from the system of GWHEs (10) and (35) after mathematical manipulation in terms of the quantities $\hat{V}_d(w) = \sin w V_+(-k\cos w)$ and $\hat{I}_+(w) = I_+(-k\cos w)$. The mapping $\eta = -k\cos w$ is described for example in Appendix I of [28] with the definition of proper and improper plane according to the multivariate function $\tau_1(\eta)$. Starting from (10) we obtain in w plane:

$$-Y_o \sin w \hat{V}_+(w) - \hat{I}_+(w) = -\hat{I}_{a+}(w+\Phi) \qquad (74)$$

as $m = kcos(w+\Phi)$. Since plus unknowns (axial spectra) are even functions in w [26], we can eliminate the minus function (face spectrum) and get a difference equation with plus unknowns. In fact by replacing w with $w-\Phi$

$$-Y_o \sin(w-\Phi)\hat{V}_+(w-\Phi) - \hat{I}_+(w-\Phi) = -\hat{I}_{a+}(w) \quad (75)$$

and considering now $\hat{I}_{a+}(w) = \hat{I}_{a+}(-w)$ we get

$$-Y_o \sin(w)\hat{V}_+(w) - \hat{I}_+(w) = Y_o \sin(w+2\Phi)\hat{V}_+(w+2\Phi) - \hat{I}_+(w+2\Phi) \qquad (76)$$

after replacing again w with $w+\Phi$.

Starting from (35) we obtain in w plane:

$$\hat{Y}_d(w)\hat{V}_+(w) + \hat{I}_+(w) = \hat{\psi}^i_+(w) + \hat{\psi}_+(w) + \hat{X}_+(w+\pi) \quad (77)$$

where $\hat{Y}_d(w) = Y_d(-k\cos w)$, $\hat{\psi}^i_+(w) = \psi^i_+(-k\cos w)$, $\hat{\psi}_+(w) = \psi_+(-k\cos w)$, $\hat{X}_+(w) = X_+(-k\cos w)$ with $X_+(-\eta) = \psi_-(\eta)$. Using the same procedure already applied in (10) we eliminate the minus unknown and we get a difference equation with plus unknowns:

$$\begin{aligned} &\hat{Y}(w)\hat{V}_+(w) + \hat{I}_+(w) - \hat{\psi}^i_+(w) - \hat{\psi}_+(w) = \\ &= \hat{Y}(-w-2\pi)\hat{V}_+(w+2\pi) + \hat{I}_+(w+2\pi) + \\ &-\hat{\psi}^i_+(w+2\pi) - \hat{\psi}_+(w+2\pi) \end{aligned} \qquad (78)$$

Since $\hat{\psi}_+(w+2\pi) = \hat{\psi}_+(w)$ and $\hat{\psi}^i_+(w+2\pi) = \hat{\psi}^i_+(w)$ we can eliminate the functions $\hat{\psi}_+(\cdot)$ and $\hat{\psi}^i_+(\cdot)$ in (78).

Finally the system of equations (76) and (78) yields the recursive equations (79) for $\hat{V}_+(w)$ and $\hat{I}_+(w)$ that are suitable to extend in the whole w plane the approximated spectra obtained from (52) via (58) taking into account the effect of the singularity lines in $-\pi < w < 0$ and considering the symmetry properties of plus functions that are even in w.

REFERENCES

[1] D.S. Jones, "A simplifying technique in the solution of a class of diffraction problems," *Quart. J. Math.*, vol. 3, n. 2 , pp.189-196, 1952.

[2] D.S. Jones, "Diffraction by a waveguide of finite length," Proc. Cambridge Phil. Soc., vol. 48, pp. 118-134, 1952.

[3] B.Noble, *Methods Based on the Wiener-Hopf Technique: For the Solution of Partial Differential Equations,* London, UK:Pergamon, 1958.

[4] D.S. Jones, *The theory of electromagnetism,* Oxford, UK: Pergamon Press, 1964.

[5] R. Mittra, S.W. Lee, *Analytical Techniques in the Theory of Guided Waves,* New York: The MacMillan Company, 1971.

[6] K. Kobayashi, "On the Factorization of certain kernels arising in functional equations of the Wiener-Hopf type," *Journal of the Physical Society of Japan,* 53, pp. 2885-2898, 1984,

[7] K. Kobayashi, "Diffraction of a plane electromagnetic wave by a parallel plate grating with dielectric loading: The case of transverse magnetic incidence," *Can. J. Phys.,* vol. 63, pp. 453-465, 1985.

[8] A. Büyükaksoy, A.H. Serbest, "Matrix Wiener-Hopf Factorization Methods and Applications to Some Diffraction Problems," ch.6 in M. Hashimoto, M.Idemen and O.A. Tretyakov Editors, *Analytical and Numerical Methods in Electromagnetic Wave Theory,* Science House Co.,Ltd., Tokio, 1993.

[9] K. Kobayashi, "Some Diffraction problems involving modified Wiener-Hopf geometries," ch.4 in M. Hashimoto, M.Idemen and O.A. Tretyakov Editors, *Analytical and Numerical Methods in Electromagnetic Wave Theory,* Science House Co.,Ltd., Tokio, 1993.

[10] V. Daniele, R. Zich, *The Wiener-Hopf method in electromagnetics,* Raleigh, NC: SciTech Publishing, 2014

[11] G. Cinar, A. Buyukaksoy, "Diffraction on a normally incident plane wave by three parallel half-planes with different face impedances," *IEEE Trans. Antennas Propag.,* vol. 52, pp.478-486, 2004.

[12] Y.A. Antipov, V.V. Silvestrov, "Electromagnetic scattering from an anisotropic half-plane at oblique incidence: the exact solution," *Quart. J. Mech. Appl. Math.,* vol. 59, 211-251, 2006.

[13] E. H. Shang, K. Kobayashi, "Diffraction by a terminated, semi-infinite parallel-plate waveguide with four-layer material loading," *Progress In Electromagnetics Research B,* n. 12, pagg. 1-33, 2009.

[14] A.D. Rawlins, "The method of finite-product extraction and an application to Wiener-Hopf theory," *IMA J. Appl. Math.,* vol 77, n.4, pp. 590-602, 2012.

[15] R. Nawaz, M. Ayub, "An exact and asymptotic analysis of a diffraction problem,", *Meccanica,* vol. 48, n. 3, pp. 653-662, 2013.

[16] K. Kobayashi, "Solutions of wave scattering problems for a class of the modified wiener-hopf geometries," *IEEJ Transactions on Fundamentals and Materials,* vol. 133, n. 5, pagg. 233-241, 2013.

[17] R. Nawaz, A. Naeem, M. Ayub, A. Javaid, "Point source diffraction by a slit in a moving fluid," *Waves in Random and Complex Media,* vol. 24, n. 4, pp. 357-375, 2014.

$$\begin{aligned}\hat{V}_+(w) &= \frac{\hat{V}_+(w+2\Phi)\sin(w+2\Phi)+Z_o\hat{V}_+(w+2\pi)\hat{Y}_d(-w-2\pi)-Z_o\hat{I}_+(w+2\Phi)+Z_o\hat{I}_+(w+2\pi)}{Z_o\hat{Y}_d(w)-\sin w}\\ \hat{I}_+(w) &= \frac{\hat{Y}_d(w)\hat{V}_+(w+2\Phi)\sin(w+2\Phi)+\hat{V}_+(w+2\pi)\hat{Y}_d(-w-2\pi)\sin(w)-Z_o\hat{Y}_d(w)\hat{I}_+(w+2\Phi)+\hat{I}_+(w+2\pi)\sin(w)}{\sin(w)-Z_o\hat{Y}_d(w)}\end{aligned} \tag{79}$$

[18] D.G. Crowdy, E. Luca, "Solving Wiener-Hopf problems without kernel factorization," *Proc. R. Soc. Lond. Ser. A Math. Phys. Eng. Sci.,* vol. 470, n. 2170, art. no. 20140304, 20 pp. 2014.

[19] S. Rogosin, G. Mishuris, "Constructive methods for factorization of matrix-functions," *IMA J. Appl. Math.,* vol.81, n. 2, pp. 365-391, 2016.

[20] G. Fusai, G. Germano, D. Marazzina,"Spitzer identity, Wiener-Hopf factorization and pricing of discretely monitored exotic options," *European Journal of Operational Research,* vol. 251, n.1, pp. 124-134, 2016.

[21] D. Margetis, M. Maier, M. Luskin, "On the Wiener-Hopf Method for Surface Plasmons: Diffraction from Semiinfinite Metamaterial Sheet," *Studies in Applied Mathematics,* vol. 139, n. 4, pp. 599-625, 2017.

[22] T. Nagasaka e K. Kobayashi, "Wiener-Hopf analysis of the planewave diffraction by a thin material strip: The case of e polarization," *IEICE Transactions on Electronics,* vol. E101C, n. 1, pagg. 12-19, 2018.

[23] A. Kisil, L.J. Ayton, "Aerodynamic noise from rigid trailing edges with finite porous extensions," *J Fluid Mech,* vol. 836, pp. 117-144, 2018.

[24] J.B. Lawrie, I.D. Abrahams, "A brief historical perspective of the Wiener-Hopf technique," *J. Eng. Mat.,* vol. 59:4, pp. 351-358, 2007.

[25] V.G. Daniele, G. Lombardi, R.S. Zich, "The Double PEC Wedge Problem: Diffraction and Total Far Field," *Trans. Antennas Propagat.,* vol. 66, n. 12, pp. 6470-6673, 2018, doi: 10.1109/TAP.2018.2877260.

[26] V. Daniele, "The Wiener-Hopf technique for impenetrable wedges having arbitrary aperture angle," *SIAM Journal of Applied Mathematics,* vol.63, n.4, pp. 1442-1460, 2003.

[27] V.G. Daniele and G. Lombardi, "The Wiener-Hopf technique for impenetrable wedge problems," in Proc. of Days on Diffraction Internat. Conf., invited paper, pp. 50-61, Saint Petersburg, Russia, June 2005.

[28] V. Daniele, and G. Lombardi, "Wiener-Hopf Solution for Impenetrable Wedges at Skew Incidence," *IEEE Trans. Antennas Propagat.,* vol. 54, n. 9, pp. 2472-2485, Sept. 2006.

[29] V. Daniele, "The Wiener-Hopf formulation of the dielectric wedge problem: Part I," *Electromagnetics*, vol. 30, n. 8, pp. 625-643, 2010.

[30] V. Daniele, "The Wiener-Hopf formulation of the dielectric wedge problem: Part II," *Electromagnetics*, vol. 31, n. 1, pp. 1-17, 2011.

[31] V. Daniele, "The Wiener-Hopf formulation of the dielectric wedge problem. Part III: The skew incidence case," *Electromagnetics*, vol. 31, n. 8, pp. 550-570, 2011.

[32] V. Daniele, and G. Lombardi, "The Wiener-Hopf Solution of the Isotropic Penetrable Wedge Problem: Diffraction and Total Field," IEEE Trans. Antennas Propagat., vol. 59, n. 10, pp. 3797-3818, Oct. 2011.

[33] G. Lombardi, "Skew Incidence on Concave Wedge With Anisotropic Surface Impedance," *IEEE Antennas Wireless Propag. Lett.,* vol. 11, pp. 1141-1145, 2012

[34] B. Budaev, *Diffraction by wedges,* London, UK: Longman Scient., 1995.

[35] T.B.A. Senior, and J.L. Volakis, *Approximate boundary conditions in electromagnetics,* London, UK: IEE, 1995.

[36] J. M. L. Bernard, "Diffraction at skew incidence by an anisotropic impedance wedge in electromagnetism theory: A new class of canonical cases," *J. Physics A: Math. Gen.,* vol. 31, no. 2, pp. 595-613, 1998.

[37] J.M.L. Bernard, "A spectral approach for scattering by impedance polygons," *Quart. J. Math.,* Vol. 59, n. 4, pp. 517-550, 2006.

[38] V.M. Babich, M.A. Lyalinov, and V.E. Grikurov, *Sommerfeld-Malyuzhinets Technique in Diffraction Theory,* Oxford, UK: Alpha Science, 2007.

[39] D.S. Jones, *The theory of electromagnetism,* Oxford, UK: Pergamon Press, 1964.

[40] A.V. Osipov, "On the method of Kontorovich-Lebedev integrals in problems of wave diffraction in sectorial media," in *Problems of diffraction and propagation of waves*, Vol. 25, pp. 173-219, St Petersburg University Publications, 1993.

[41] M.A. Salem, A. Kamel, and A.V. Osipov, "Electromagnetic fields in the presence of an infinite dielectric wedge," *Proc. Royal Society Math., Phys. Engrng. Sci.,* vol. 462, pp. 2503-2522, 2006.

[42] V.G. Daniele, "Electromagnetic fields for PEC wedge over stratified media. Part I," *Electromagnetics*, vol. 33, pp. 179-200, 2013.

[43] V.G. Daniele, G. Lombardi, "Arbitrarily oriented perfectly conducting wedge over a dielectric half-space: diffraction and total far field," *IEEE Trans. Antennas Propag.,* vol. 64, n. 4, pp. 1416-1433, 2016.

[44] V.G. Daniele, G. Lombardi, R.S. Zich, "Network representations of angular regions for electromagnetic scattering," *Plos One,* vol. 12, n. 8, e0182763, pp. 1-53, 2017, https://doi.org/10.1371/journal.pone.0182763.

[45] V.G. Daniele, G. Lombardi, R.S. Zich, "The electromagnetic field for a PEC wedge over a grounded dielectric slab: 1. Formulation and validation," *Radio Science,* vol. 52, pp. 1472-1491, 2017.

[46] V.G. Daniele, G. Lombardi, R.S. Zich, "The electromagnetic field for a PEC wedge over a grounded dielectric slab: 2. Diffraction, Modal Field, SurfaceWaves, and Leaky Waves," *Radio Science,* vol. 52, pp. 1492-1509, 2017.

[47] V.G. Daniele, G. Lombardi, R.S. Zich, "The scattering of electromagnetic waves by two opposite staggered perfectly electrically conducting half-planes," *Wave Motion,* vol. 83, pp. 241-263, 2018, doi: 10.1016/j.wavemoti.2018.09.017

[48] L. B. Felsen and N. Marcuvitz, *Radiation and Scattering of Waves,* Englewood Cliffs, NJ: Prentice-Hall, 1973.

[49] V.G.Daniele, and G.Lombardi,"Fredholm Factorization of Wiener-Hopf scalar and matrix kernels," *Radio Science,* vol. 42,RS6S01,pp.1-19, 2007

[50] L.V. Kantorovich and V.I. Krylov, *Approximate methods of higher analysis,* Groningen, The Netherlands: Noordhoff, 1964.

[51] V.G. Daniele, R.D. Graglia, G. Lombardi, P.L.E. Uslenghi, "Cylindrical resonator sectorally filled with DNG metamaterial and excited by a line source," *IEEE Antennas Wireless Propag. Lett.,* vol. 11, pp. 1060-1063, 2012.

[52] S.-W. Lee, R. Mittra, "Diffraction by Thick Conducting Haft-Plane and a Dielectric-Loaded Waveguide," *IEEE Trans. Antennas Propag.,* vol. 16, n. 4, pp. 454-461, 1968.

[53] M.F. Iskander, M.A.K. Hamid, "Scattering coefficients at a waveguide-horn junction," *Proc. of the IEE,* vol. 123, n. 2, pp. 123-127, 1976.

[54] S. Maci, P.Y. Ufimtsev, R. Tiberio, "Equivalence between physical optics and aperture integration for radiation from open-ended waveguides," *IEEE Trans. Antennas Propag.,* vol. 45, n. 1, pp. 183-185, 1997.

[55] E.L. Shenderov, "Diffraction of a sound wave by the open end of a flanged waveguide with impedance walls." *Acoustical Physics, vol. 46,* n. 6, pp. 716-727, 2000.

[56] H.T. Anastassiu, "A review of electromagnetic scattering analysis for inlets, cavities, and open ducts," *IEEE Antennas Propag. Mag.,* vol. 45, n. 6, pp. 27-40, 2003.

[57] H. Serizawa, K. Hongo, "Radiation from a flanged rectangular waveguide," *IEEE Trans. Antennas Propag.,* vol. 53, n. 12, pp. 3953-3962, 2005.

[58] W. Tan, Z. Shen, "An accelerating technique for analyzing open-ended rectangular waveguides," *Microwave and Optical Technology Letters,* vol. 50, n. 4, pp. 1061-1066, 2008.

[59] J.-H. Kim, B. Enkhbayar, J.-H. Bang, B.-C. Ahn, E.-J. Cha, " New formulas for the reflection coefficient of an open-ended rectangular waveguide radiating into air including the effect of wall thickness or flange," *PIER M,* vol. 12, pp. 143-153, 2010.

[60] Y.H. Cho, " Analytic and numerically efficient scattering equations for an infinitely flanged coaxial line," *PIER Letters,* vol. 28, pp. 149-158, 2012.

[61] Y. Abe, H. Shirai, R. Sato, "High frequency asymptotic analysis of modal excitation at flanged parallel plane waveguides," in 2012 Fourth International Conference on Communications and Electronics (ICCE), Hue, Vietnam, pp. 377-380, 2012.

[62] P. L. E. Uslenghi, "Electromagnetic Scattering by Metallic Cylinders Perpendicularly Truncated by a Metal Plane," *IEEE Trans. Antennas Propag.,* vol. 63, no. 5, pp. 2228-2236, May 2015.

[63] J. Meixner, "The behavior of electromagnetic fields at edges," *IEEE Trans. Antennas Propag.,* 20, 442-446 (1972).

[64] R.D. Graglia and G. Lombardi, "Singular higher order complete vector bases for finite methods," *IEEE Trans. Antennas Propag.,* vol. 52, no. 7, pp. 1672-1685, Jul. 2004.

[65] R. D. Graglia, G. Lombardi, D. R. Wilton and W. A. Johnson, "Modeling edge singularities in the method of moments," *Proc. IEEE AP-S Int. Symp.,* Washington, DC, 2005, pp. 56-59 vol. 3A.

[66] R. D. Graglia and G. Lombardi, "Singular higher order divergence-conforming bases of additive kind and moments method applications to 3D sharp-wedge structures," *IEEE Trans. Antennas Propag.,* vol. 56, no. 12, pp. 3768-3788, Dec. 2008.

[67] B. Friedman, *Principles and Techniques of Applied Mathematics,* Ch. 3, p.167, John Wiley & Sons, 1956

[68] F. Gakhov, *Boundary value problems,* Ch. 9, Dover Publications, 1990

[69] V.G. Daniele, "Rotating Waves in the Laplace Domain for Angular Regions," *Electromagnetics,*, vol. 23, n. 3, pp. 223-236, 2003.

[70] R. G. Kouyoumjian and P. H. Pathak, "A uniform geometrical theory of diffraction for an edge in a perfectly conducting surface," *Proc. IEEE,* vol. 62, pp. 1448-1461, Nov. 1974.

Vito Daniele was born in Catanzaro, Italy, on March 20, 1942. He received the degree in electronic engineering from Polytechnic of Turin, Italy, in 1966. In 1980, he was appointed Full Professor in Electrical Engineering at the University of Catania. From 1981 to 2012 he was Professor of Electrical Engineering at the Polytechnic of Turin and since 2015 he is Emeritus Professor at the same Polytechnic.

He has served also as a Consultant to various industries in Italy. He has published more than 150 papers in refereed journals and conference proceedings and several textbook chapters.

His research interests are mainly in analytical and approximate techniques for the evaluation of electromagnetic fields both in high and in low frequency. In particular his studies on the Wiener Hopf technique have produced the recent book "The Wiener-Hopf Method in Electromagnetics". Prof. Daniele was the Guest Editor of a special issue on Electromagnetic Coupling to Transmission Lines for Electromagnetics in 1988, Chairman and Invited Speaker for several international symposia, and reviewer for many international journals.

Since 2013 he is corresponding Member of the Academy of Sciences of Torino.

Guido Lombardi (S'02-M'03-SM'11-) was born in Florence, Italy, on December 8, 1974. He received the Laurea degree (*summa cum laude*) in telecommunications engineering from the University of Florence, Italy, in 1999 and the Ph.D. degree in electronics engineering at the Polytechnic of Turin, Italy, in jan. 2004. In 2000-01, he was officer of the Italian Air Force. In 2004 he was an Associate Researcher with the Department of Electronics of Polytechnic of Turin and in 2005 he joined the same Department as an Assistant Professor with tenure and where he is currently an Associate Professor. He was the recipient of the Raj Mittra Travel Grant award for junior researcher at 2003 IEEE AP-S International Symposium and USNC/CNC/URSI National Radio Science Meeting, Columbus, OH, USA. In the same year he was Visiting Researcher at the Department of Electrical and Computer Engineering, University of Houston, Houston, TX, USA. In 2018 he was recipient of the London Mathematical Society Research in Pairs grant as research visitor to the University of Cambridge, UK. His research interests comprise analytical and numerical methods for electromagnetics, Wiener-Hopf method, diffraction, theoretical and computational aspects of FEM and MoM, numerical integration, electromagnetic singularities, waveguide problems, microwave passive components, project of orthomode transducers (OMT), metamaterials. He was an associate editor of the IEEE Trans. Antennas Propagat (2016-19) where currently serves as Track Editor (2019-). He is an associate editor of the IEEE ACCESS journal and the IET Electronics Letters. He is an IEEE APS AdCom member for the triennium (2016-18) and (2019-21). He served as member of the Organizing Committee in the International Conference on Electromagnetics in Advanced Applications (ICEAA) since the 2001 edition and in the IEEE-APS Topical Conference on Antennas and Propagation in Wireless Communications (IEEE-APWC) since the 2011 edition. He was Publication Chair of ICEAA and IEEE-APWC since 2011 edition. He was AP-S Technical Program Vice-Chair (Propagation and Scattering) at the 2019 IEEE AP-S International Symposium and USNC/CNC/URSI National Radio Science Meeting, Atlanta, GA, USA. He was Programme Organizer at Newton Institute for Mathematical Sciences (INI), University of Cambridge, UK, August 5-30, 2019. He served the 2012 and 2015 IEEE AP-S International Symposium and USNC/CNC/URSI National Radio Science Meeting, Chicago, IL, USA as co-organizer of the Special Sessions on innovative analytical and numerical techniques for complex scattering problems, special materials, nanostructures. He regularly serves as a reviewer of several international journals on physics, electrical engineering and electromagnetics, among which IEEE, IET, Wiley, Elsevier, PLoS, ACES Journals and Transactions.

Rodolfo S. Zich (Honorary Member '16-)was born in Torino, Italy, on July 15, 1939. He graduated in Electronic Engineering at Politecnico di Torino in 1962, where he has been full professor of Electromagnetic Fields and Circuits since 1976; now Emeritus (2010). He served as Rector of Politecnico from 1987 to 2001.

He has an extensive international experience: he was member of the Board of Directors of Ecole Polytechnique de Paris (Palaiseau); President of Columbus (Association of Latin America and Europe Universities) and CLUSTER (Cooperative Link between Universities for Science, Technology for Education and Research). Very active in promoting education and applied research in cooperation with public and private partners; in 1999 he founded Istituto Superiore Mario Boella, a research center on Information and Communication Technologies (ICT).

Author of several papers, his scientific interests are mainly on hybrid analytical numerical techniques in electromagnetic scattering. Gold Medal and First Class Diploma of Merit for Science, Culture and Art (2007, Italy); member of the National Academy of Science of Turin (2001).

He was awarded the IEEE Honorary membership in 2016.